Electronic supplementary information for

Aluminum complexes with Schiff base bridged bis(indolyl) ligands: synthesis, structure, and catalytic activity for polymerization of *rac*-lactide

Yun Wei,[†] Lulu Song,[†] Ling Jiang,[†] Zeming Huang,[†] Shaowu Wang,*[,†,‡,§] Qingbing Yuan,[†] Xiaolong Mu,[†] Xiancui Zhu,[†] and Shuangliu Zhou[†]

[†]Laboratory of Functional Molecular Solids, Ministry of Education, Anhui Laboratory of Molecule-Based Materials, School of Chemistry and Materials Science, Anhui Normal University, Wuhu, Anhui 241002, P. R. China,

[‡]College of Biological and Chemical Engineering, Anhui Polytechnic University, Wuhu, Anhui 241000, P. R. China

[§] State Key Laboratory of Organometallic Chemistry, Shanghai Institute of Organic Chemistry, Chinese Academy of Sciences, Shanghai 200032, P. R. China

Table S1. Summary of crystal and refinement data for complexes 1-3

	1	**2**	**3**	**4**
formula	$C_{22}H_{21}AlN_4$	$C_{23}H_{23}AlN_4$	$C_{25}H_{27}AlN_4$	$C_{26}H_{27}AlN_4(THF)$
fw	368.41	382.43	410.48	494.60
T (K)	293(2)	293(2)	293(2)	293(2)
λ (Å)	0.71073	0.71073	0.71073	0.71073
crystal system	Monoclinic	Monoclinic	Orthorhombic	Triclinic
space group	$P2_1/c$	$P2_1/c$	$Pbca$	$P\bar{1}$
a (Å)	8.234(7)	10.266(8)	19.113(5)	8.653(4)
b (Å)	10.608(9)	19.653(2)	12.042(3)	12.459(6)
c (Å)	21.775 (2)	10.500(8)	19.188(5)	13.740(7)
α (deg)	90	90	90	68.949(6)
β (deg)	98.405(1)	107.004(1)	90	79.141(6)
γ (deg)	90	90	90	88.321(6)
v (Å^3)	1881.4(3)	2025.9(3)	4416.2(2)	1356.5(1)
Z	4	4	8	2
D_{calcd} (mg/m^3)	1.301	1.254	1.235	1.211
μ mm^{-1}	0.122	0.116	0.111	0.104
F(000)	776	808	1744	528
θ range (deg)	1.89 - 25.35	2.07 - 25.35	2.12 -25.03	1.62 – 25.00
reflections collected/ unique	18216 / 3440	15006 / 3702	38619 / 3896	12950 / 4770
R (int)	0.0328	0.0513	0.1643	0.0485
goodness-of-fit on F^2	1.039	1.021	1.040	1.038
R_1, wR_2 [$I>2\sigma(I)$]	0.0397, 0.0976	0.0460, 0.1182	0.1013, 0.1845	0.0810, 0.2181
R_1, wR_2 (all data)	0.0547, 0.1053	0.0598, 0.1277	0.1861, 0.2237	0.1224, 0.2473
Largest diff. peak and hole, e. Å^{-3}	0.226 and -0.190	0.315 and -0.272	0.587 and -0.364	0.490 and -0.288

Table S2. Summary of crystal and refinement data for complexes **4, 5** and **3a**

	5	**3a**	**3c**
formula	$C_{26}H_{27}AlN_4(0.5\ CH_2Cl_2)$	$C_{26}H_{29}AlN_4O$	$C_{32}H_{37}AlN_4O_5$
fw	464.96	440.51	584.63
T (K)	293(2)	293(2)	293(2)
λ (Å)	0.71073	0.71073	0.71073
crystal system	Monoclinic	Monoclinic	Monoclinic
space group	$P2_1$	$P2_1/c$	$P2_1$
a (Å)	9.877(3)	12.669(3)	12.880(1)
b (Å)	19.118(6)	12.633(3)	17.844(2)
c (Å)	13.864(4)	15.592(3)	15.473(2)
α (deg)	90	90	90
β (deg)	110.002(4)	105.711(2)	104.716(3)
γ (deg)	90	90	90
v (Å^3)	2460.0(1)	2402.1(1)	3439.6(6)
Z	4	4	4
D_{calcd} (mg/m^3)	1.255	1.218	1.129
μ mm^{-1}	0.213	0.109	0.100
F(000)	980	936	1240
θ range (deg)	1.56 – 27.59	1.84-27.66	2.93-25.00
reflections collected/ unique	27603 / 10977	18873/5536	49516/11718
R (int)	0.1130	0.0931	0.1400
goodness-of-fit on F^2	0.997	1.059	0.984
R_1, wR_2 [$I>2\sigma(I)$]	0.0685, 0.1554	0.1028, 0.2176	0.0701, 0.1667
R_1, wR_2 (all data)	0.1060, 0.1795	0.1979, 0.2734	0.1979, 0.2255
Largest diff. peak and hole, e. Å^{-3}	0.780 and -0.311	0.930 and -0.667	0.225 and -0.300

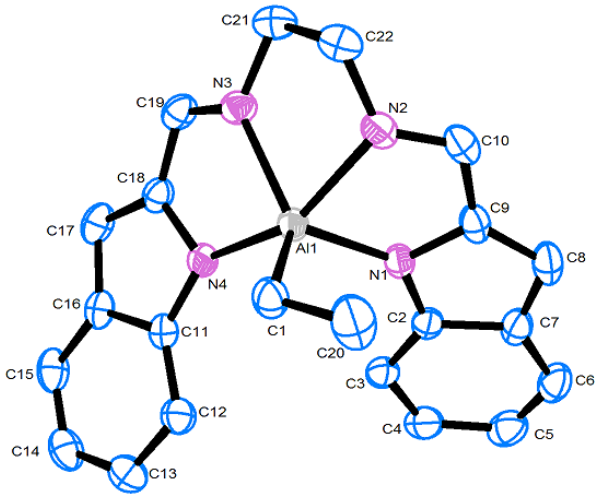

Figure S1. Molecular structure of **1**. Hydrogen atoms are omitted for clarity. Thermal ellipsoids are drawn at the 30% probability level. Selected bond length (Å) and angles (º): Al(1)-N(1) 1.938(2), Al(1)-N(2) 2.039(2), Al(1)-N(3) 2.024(2), Al(1)-N(4) 1.949(2), Al(1)-C(1) 1.968(2), N(1)-Al(1)-N(3) 121.96(7), C(1)-Al(1)-N(2) 98.7(8), N(4)-Al(1)-C(1) 103.7(8), N(4)-Al(1)-N(2) 152.9(7), C(1)-Al(1)-N(1) 109.5(8), C(1)-Al(1)-N(3) 125.3(8)

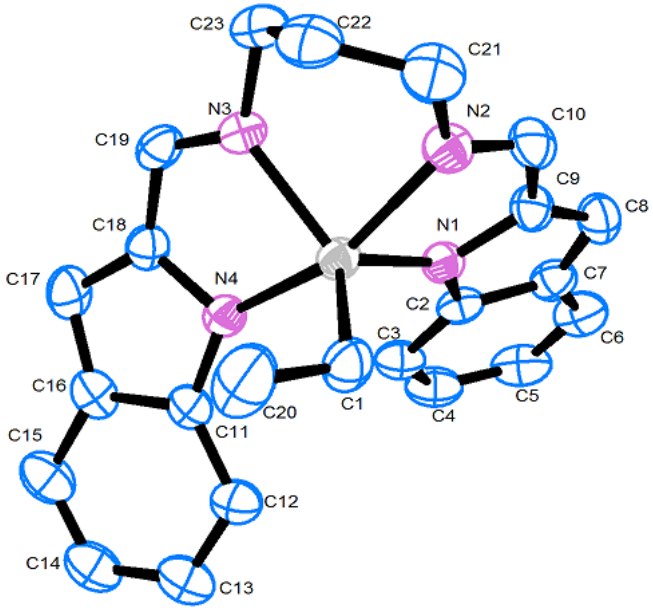

Figure S2. Molecular structure of **2**. Hydrogen atoms are omitted for clarity. Thermal ellipsoids are drawn at the 30% probability level. Selected bond length (Å) and angles (º): Al(1)-N(1) 1.924(2), Al(1)-N(2) 2.084(2), Al(1)-N(3) 2.004(2), Al(1)-N(4) 1.951(2), Al(1)-C(1) 1.967(2), N(1)-Al(1)-N(3) 118.1(7), C(1)-Al(1)-N(2) 94.8(3), N(4)-Al(1)-C(1) 100.9(3), N(4)-Al(1)-N(2) 161.7(7), C(1)-Al(1)-N(1) 118.3(3), C(1)-Al(1)-N(3) 122.1(3).

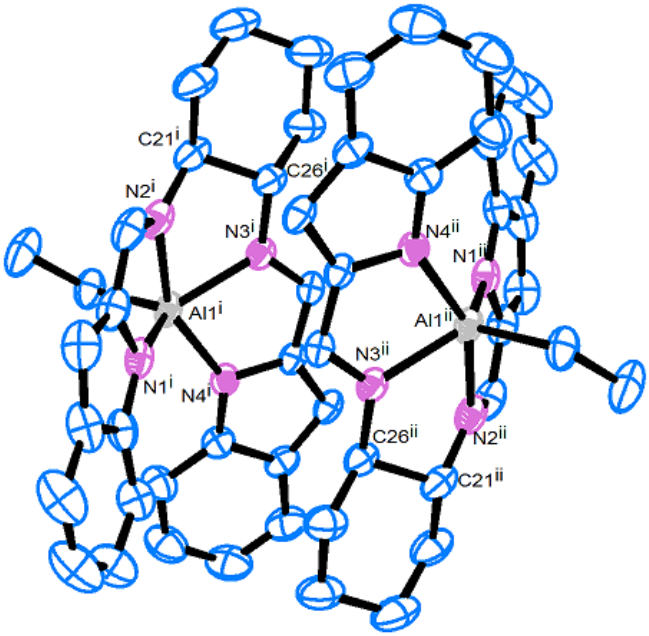

Figure S3. Molecular structure of **4**. Hydrogen atoms are omitted for clarity. Thermal ellipsoids are drawn at the 30% probability level. Selected bond length (Å) and angles (º): Al(1)-N(1) 1.948(3), Al(1)-N(2) 2.039(3), Al(1)-N(3) 2.027(3), Al(1)-N(4) 1.954(3), Al(1)-C(1) 1.961(4), N(1)-Al(1)-N(3) 123.9(2), C(1)-Al(1)-N(2) 97.9(2), N(4)-Al(1)-C(1) 104.3(2), N(4)-Al(1)-N(2) 152.4(2), C(1)-Al(1)-N(1) 114.4(2), C(1)-Al(1)-N(3) 118.0(2).

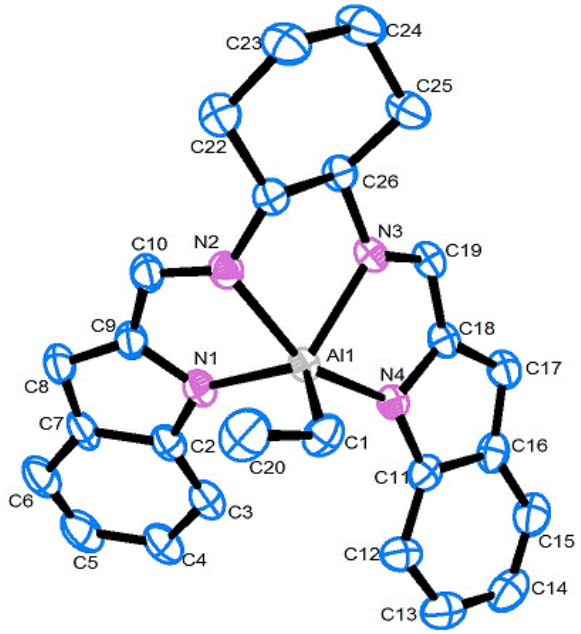

Figure S4. Molecular structure of **5**. Hydrogen atoms are omitted for clarity. Thermal ellipsoids are drawn at the 30% probability level. Selected bond length (Å) and angles (º): Al(1)-N(1) 1.950(3), Al(1)-N(2) 2.040(3), Al(1)-N(3) 2.041(3), Al(1)-N(4) 1.957(3), Al(1)-C(1) 1.975(4), N(1)-Al(1)-N(3) 123.7(2), C(1)-Al(1)-N(2) 98.5(2), N(4)-Al(1)-C(1) 103.8(2), N(4)-Al(1)-N(2) 151.8(2), C(1)-Al(1)-N(1) 114.7(2), C(1)-Al(1)-N(3) 118.0(2).

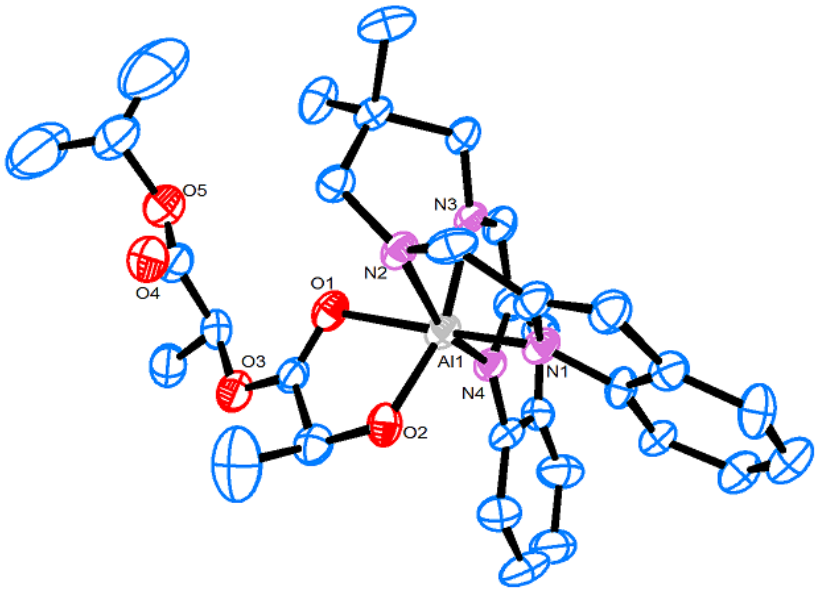

Figure S5. Molecular structure of **3c**. Hydrogen atoms are omitted for clarity. Thermal ellipsoids are drawn at the 30% probability level. Al(1)-O(1) 2.180(8), Al(1)-O(2) 1.784(7), Al(1)-N(1) 1.944(9), Al(1)-N(4) 1.923(9), Al(1)-N(2) 2.022(9), Al(1)-N(3) 2.049(9), O(1)-Al(1)-N(1) 172.4(4), O(2)-Al(1)-N(4) 100.7(4), N(4)-Al(1)-N(3) 80.3(4), N(3)-Al(1)-N(2) 79.2(4), N(2)-Al(1)-O(2) 98.7(4)

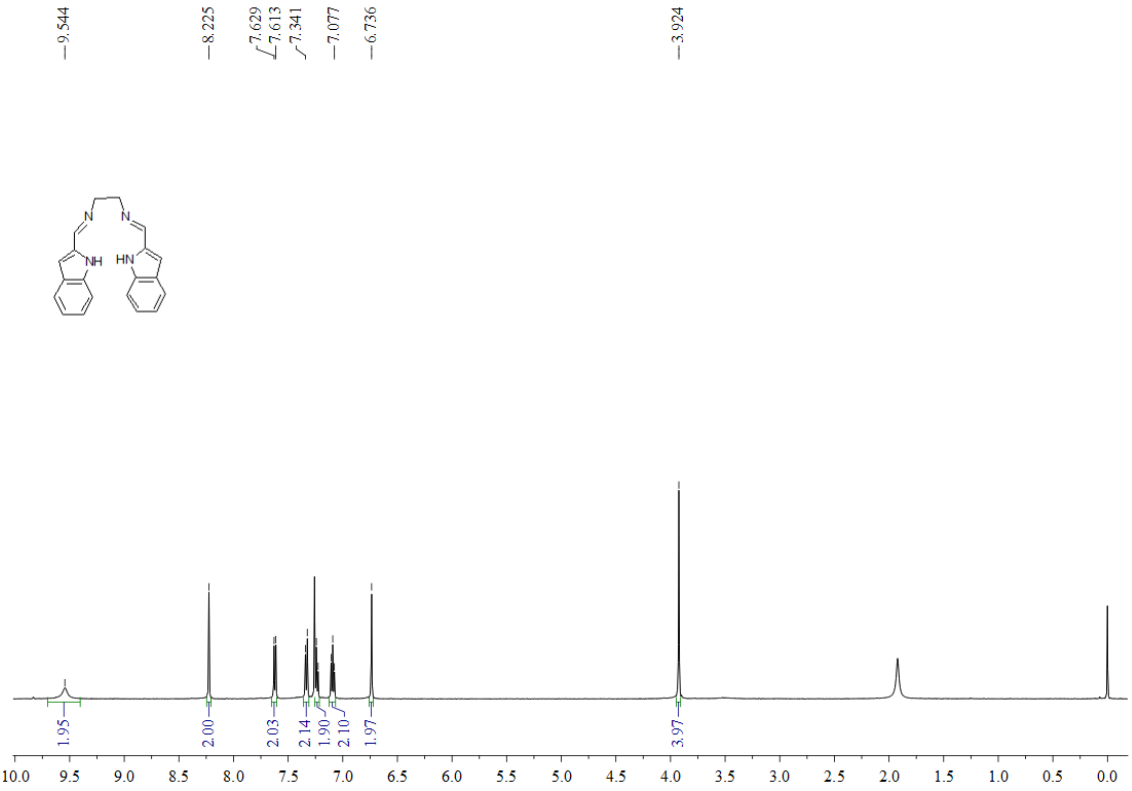

Figure S6. ^{1}H NMR spectrum (500 MHz, $CDCl_3$, 298 K) of $\mathbf{H_2L^1}$

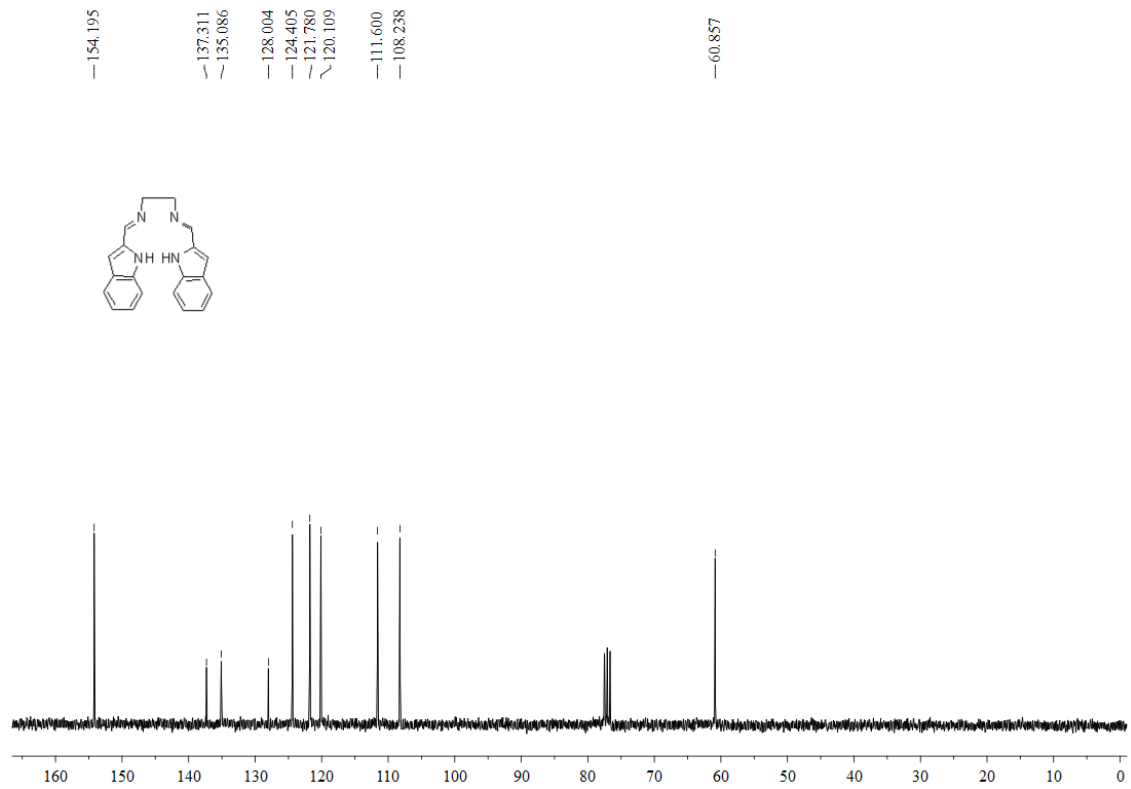

Figure S7. ^{13}C NMR spectrum (75 MHz, $CDCl_3$, 298 K) of $\mathbf{H_2L^1}$

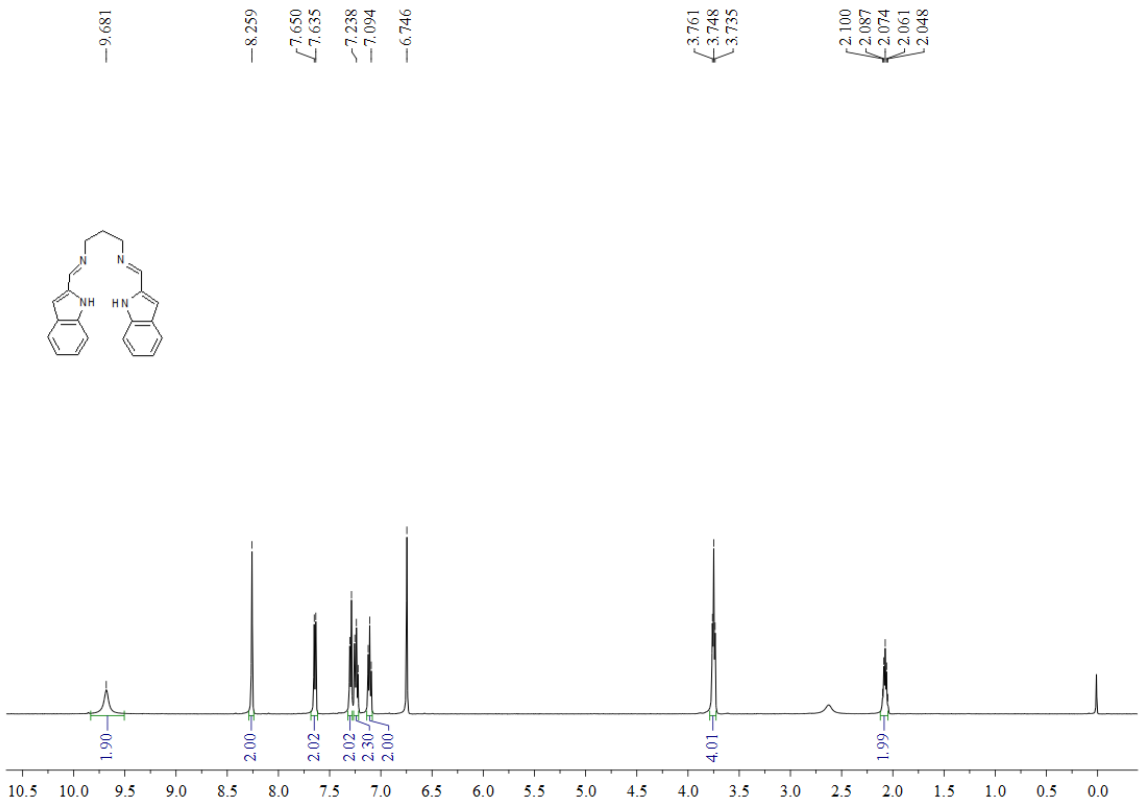

Figure S8. ^{1}H NMR spectrum (500 MHz, $CDCl_3$, 298 K) of $\mathbf{H_2L^2}$

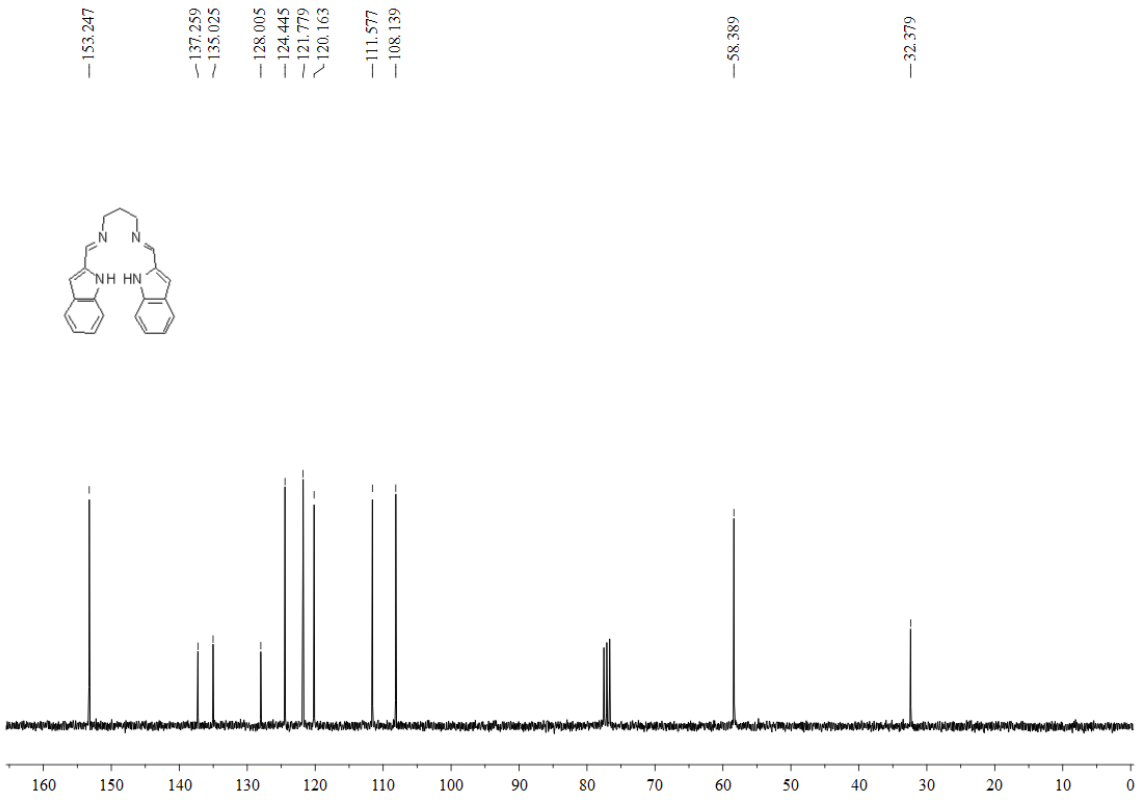

Figure S9. ^{13}C NMR spectrum (75 MHz, $CDCl_3$, 298 K) of $\mathbf{H_2L^2}$

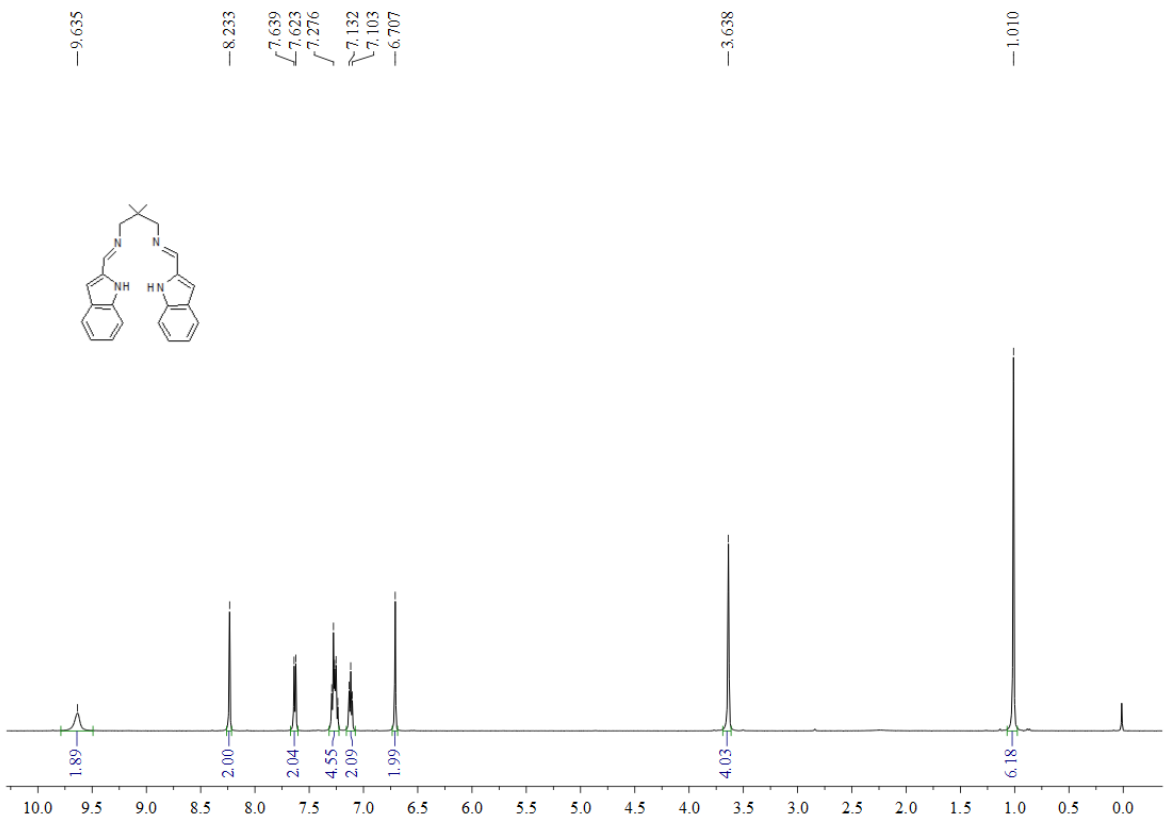

Figure S10. ^{1}H NMR spectrum (500 MHz, $CDCl_3$, 298 K) of $\mathbf{H_2L^3}$

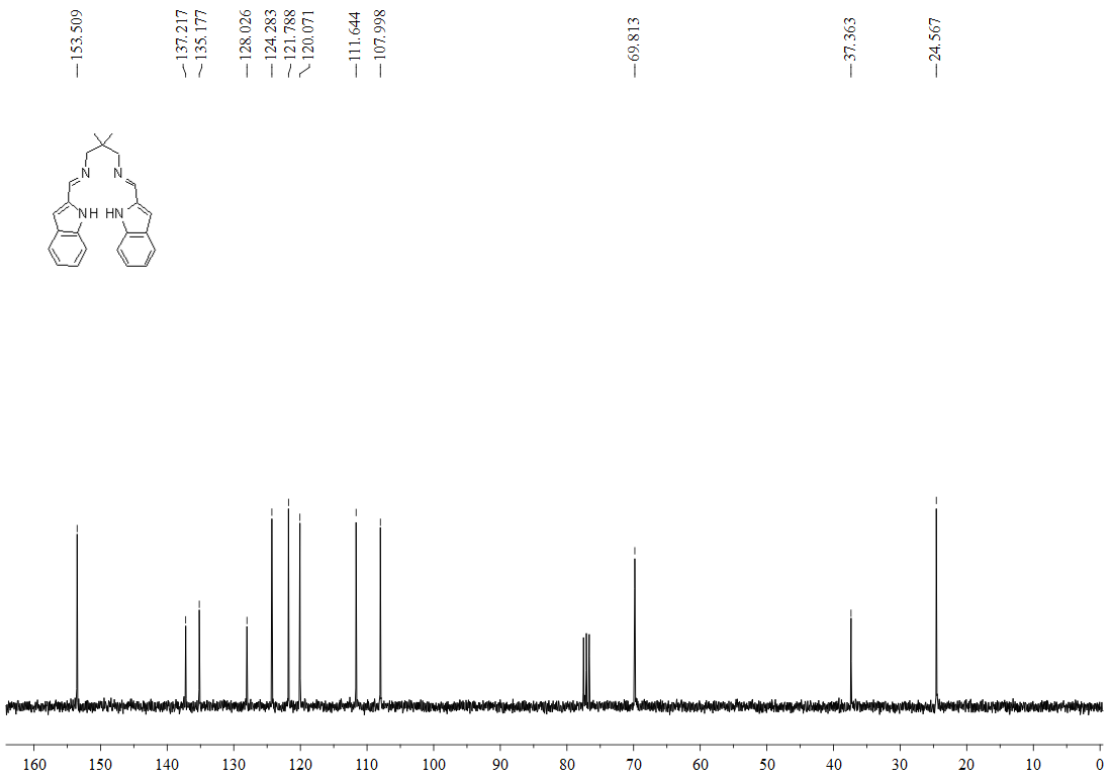

Figure S11. ^{13}C NMR spectrum (75 MHz, $CDCl_3$, 298 K) of $\mathbf{H_2L^3}$

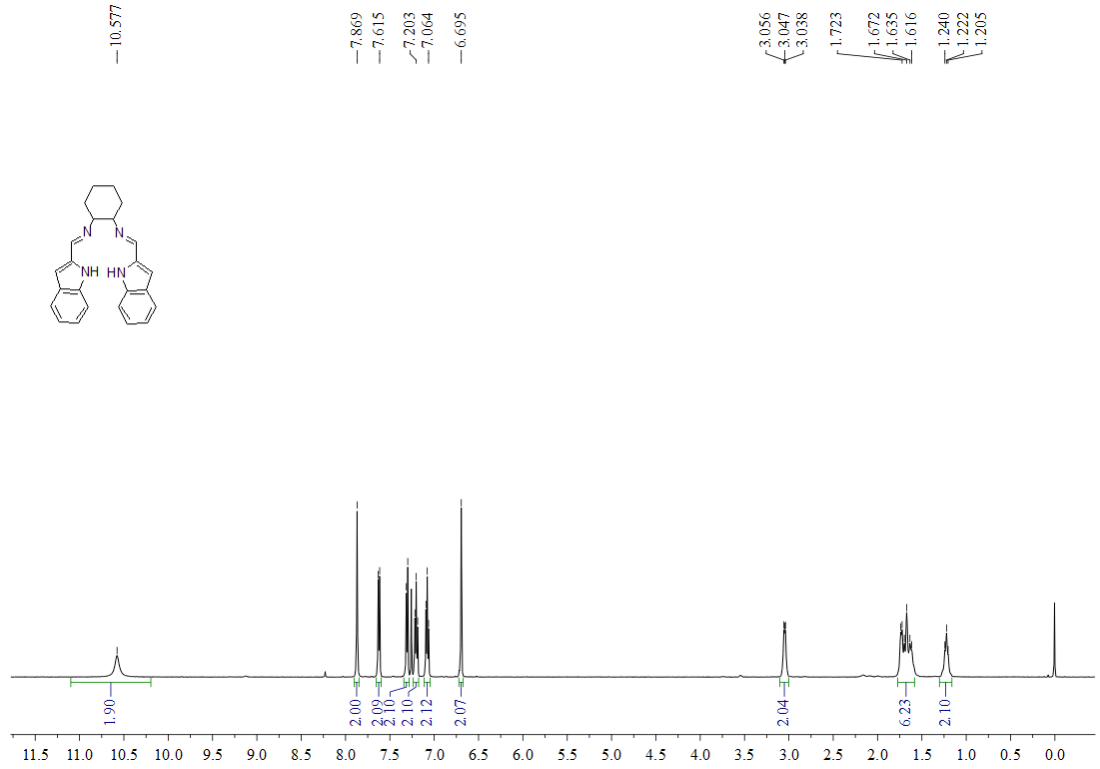

Figure S12. ^{1}H NMR spectrum (500 MHz, $CDCl_3$, 298 K) of **H_2L^4**

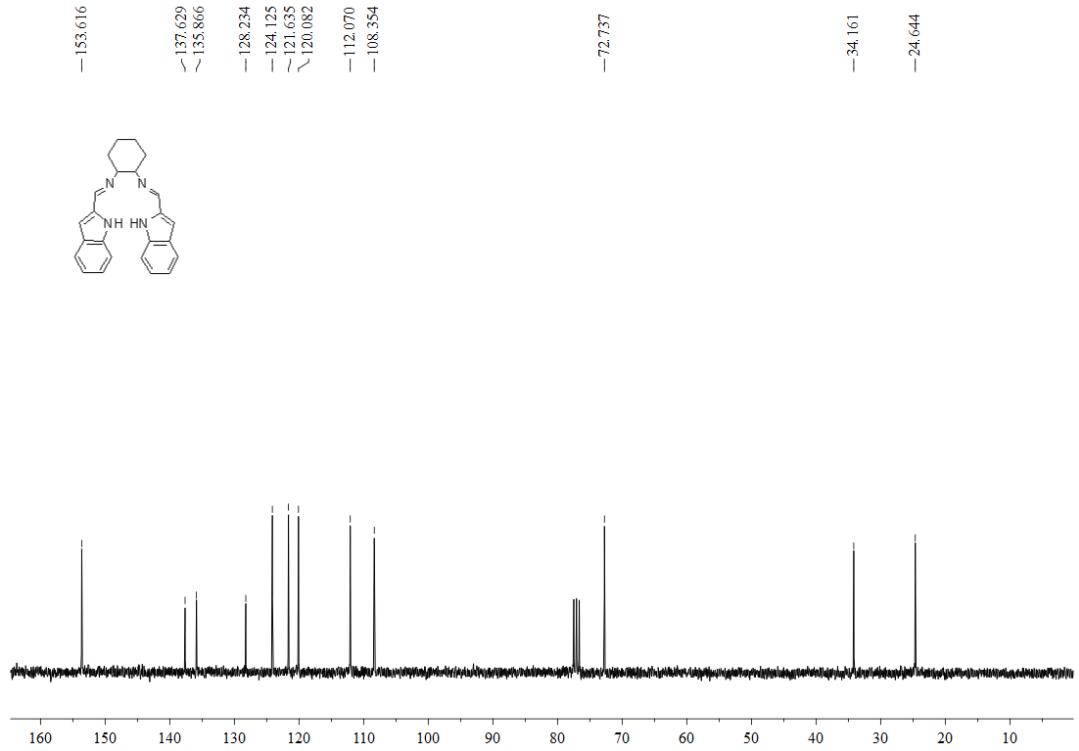

Figure S13. ^{13}C NMR spectrum (75 MHz, $CDCl_3$, 298 K) of **H_2L^4**

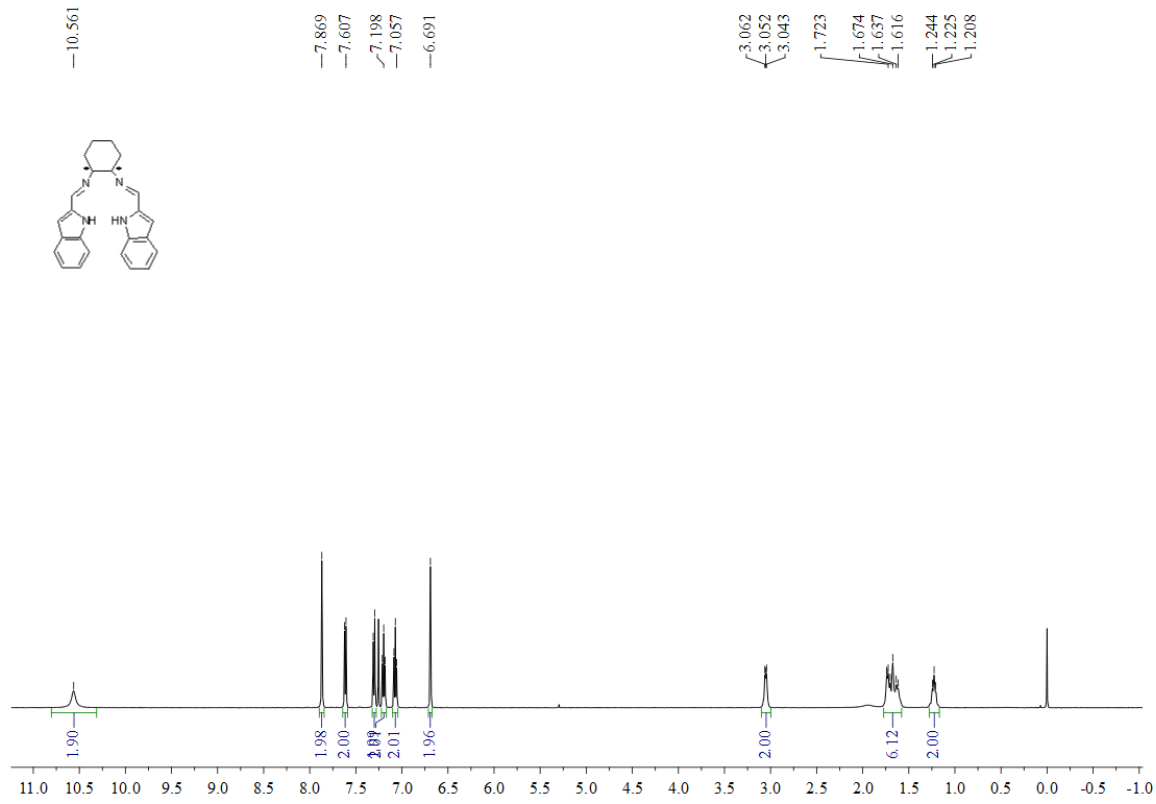

Figure S14. ^{1}H NMR spectrum (500 MHz, $CDCl_3$, 298 K) of $\mathbf{H_2L^5}$

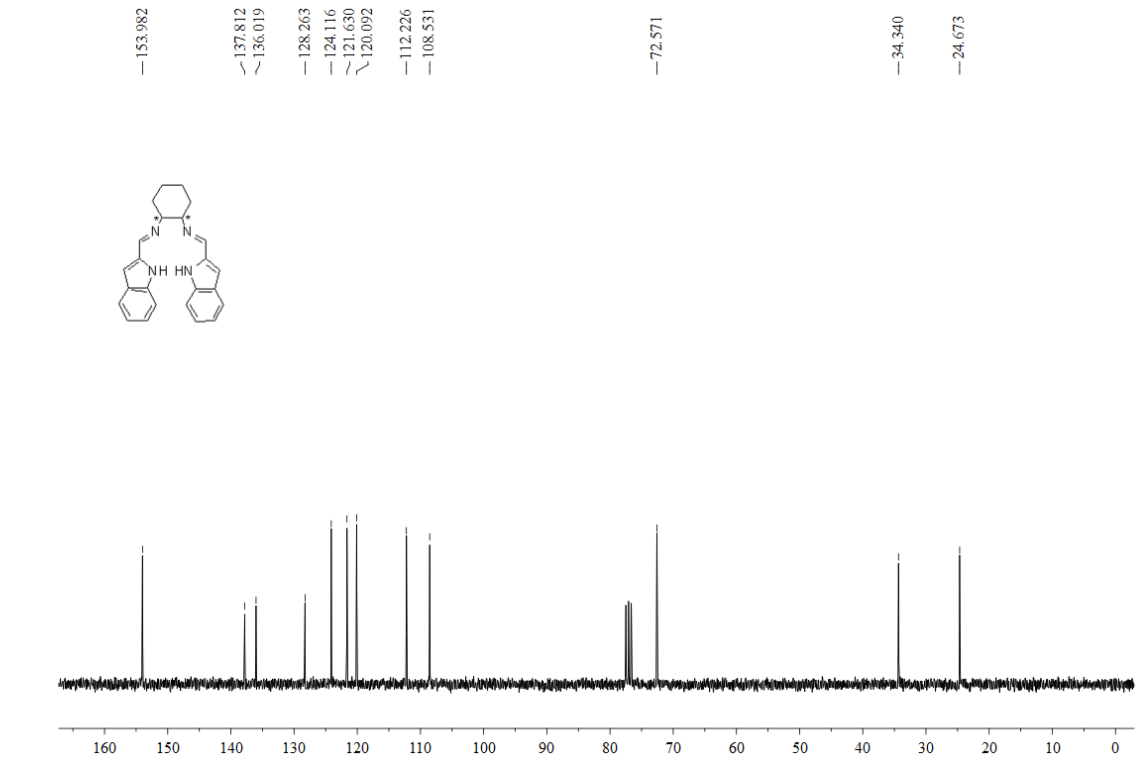

Figure S15. ^{13}C NMR spectrum (75 MHz, $CDCl_3$, 298 K) of $\mathbf{H_2L^5}$

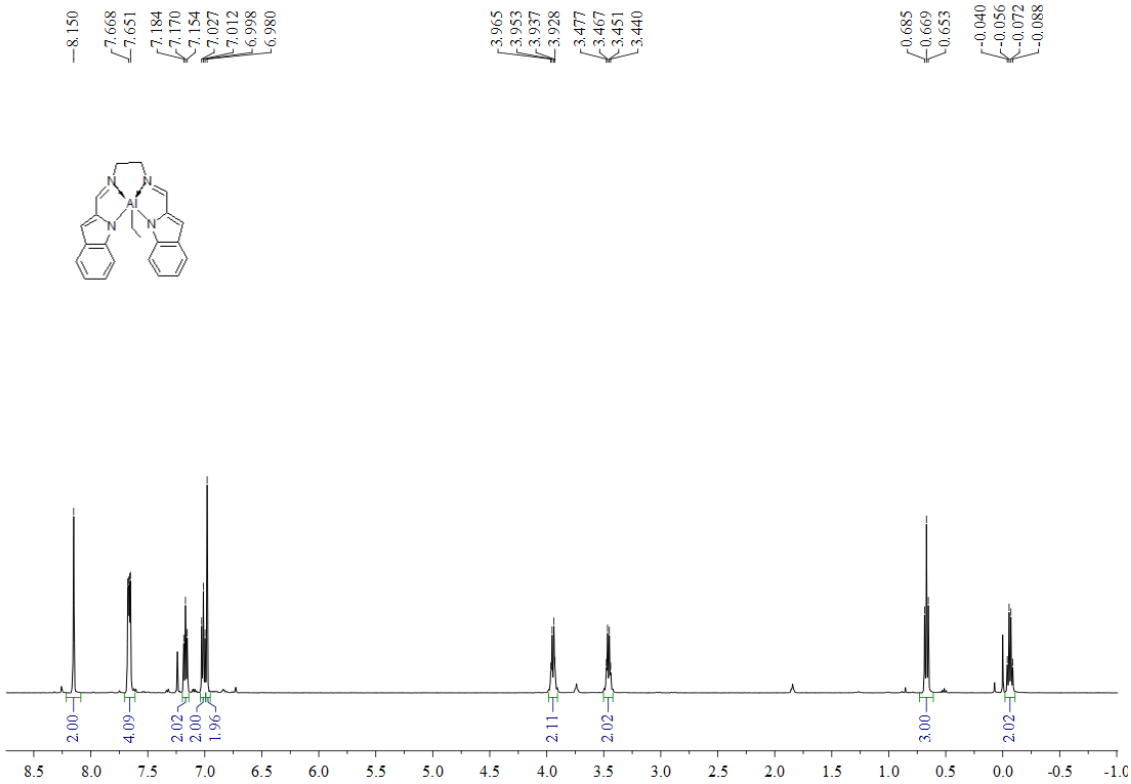

Figure S16. ^{1}H NMR spectrum (500 MHz, $CDCl_3$, 298 K) of complex **1**

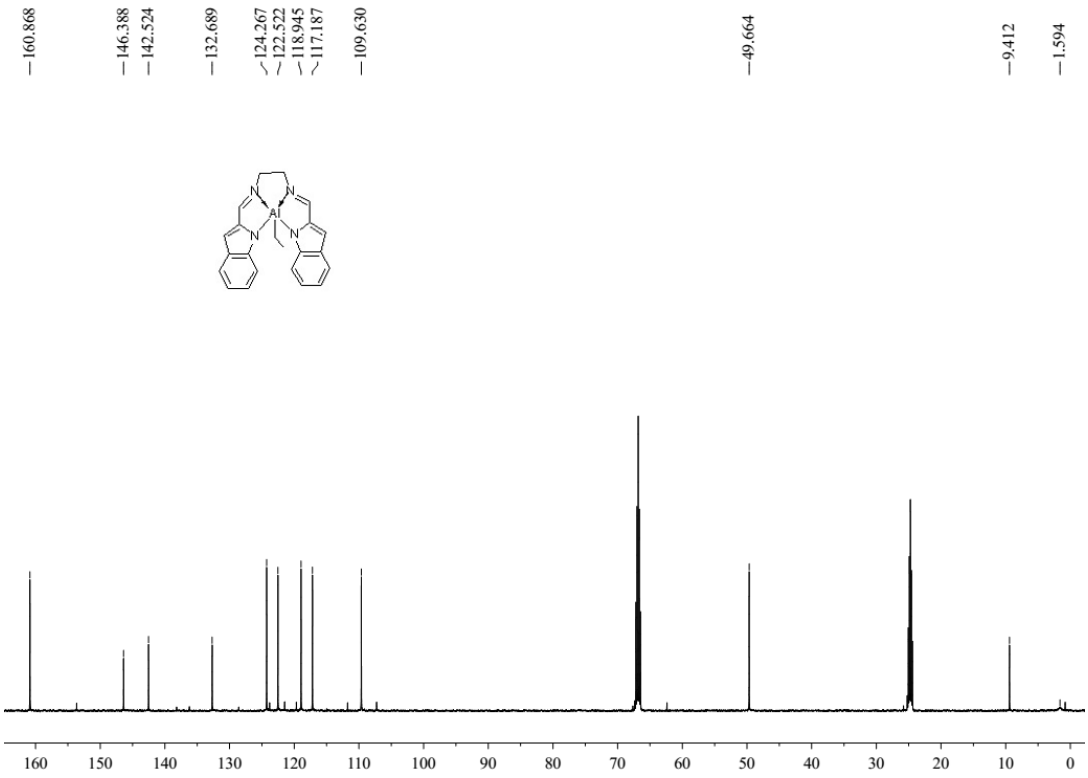

Figure S17. ^{13}C NMR spectrum (125 MHz, THF-d_8, 298 K) of complex **1**

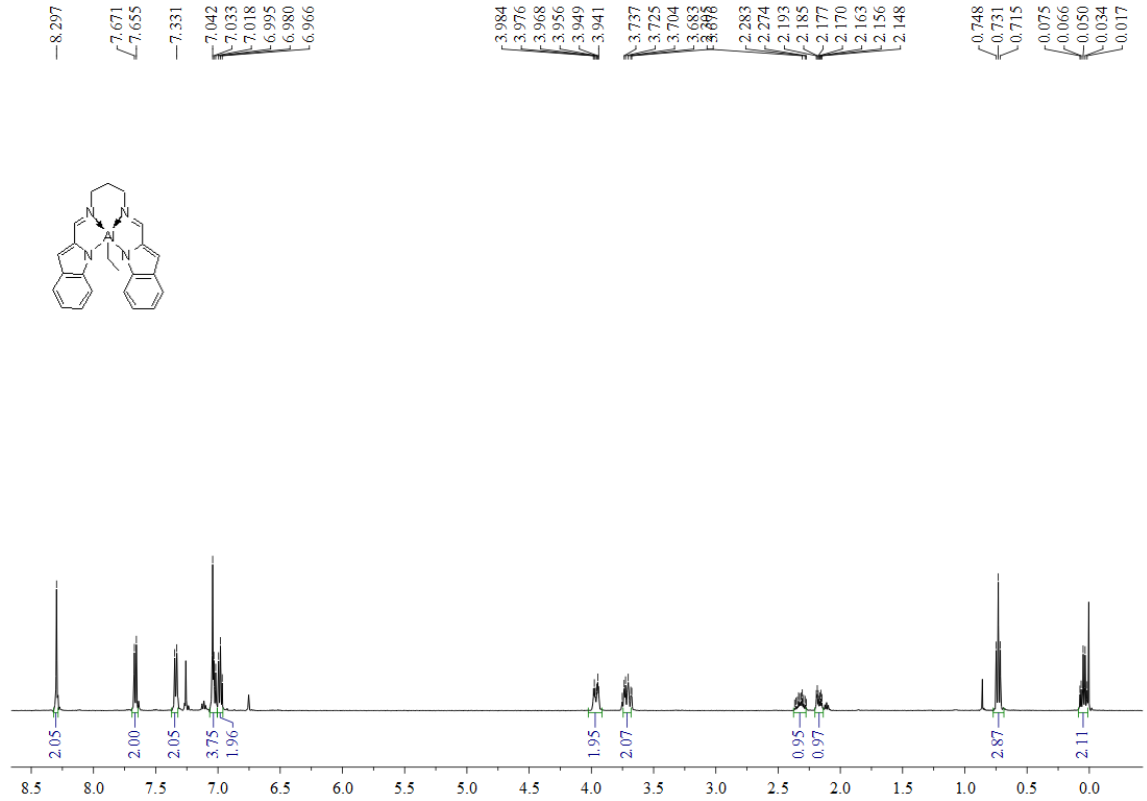

Figure S18. ^{1}H NMR spectrum (500 MHz, $CDCl_3$, 298 K) of complex **2**

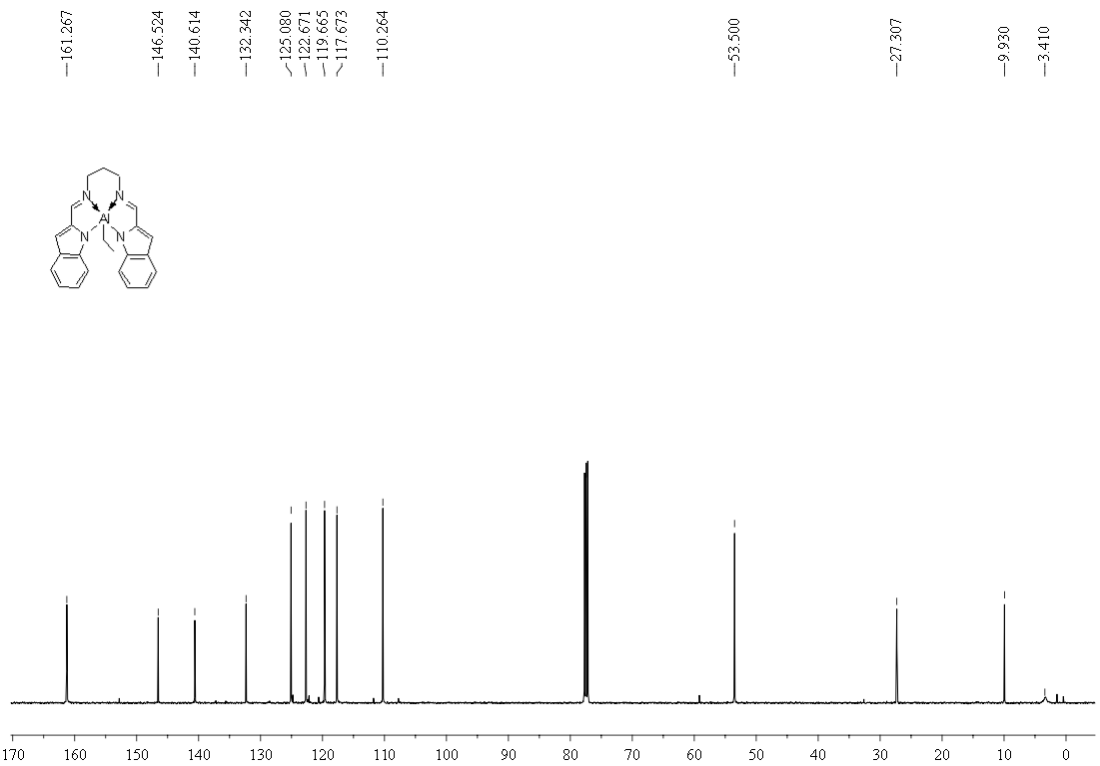

Figure S19. ^{13}C NMR spectrum (125 MHz, $CDCl_3$, 298 K) of complex **2**

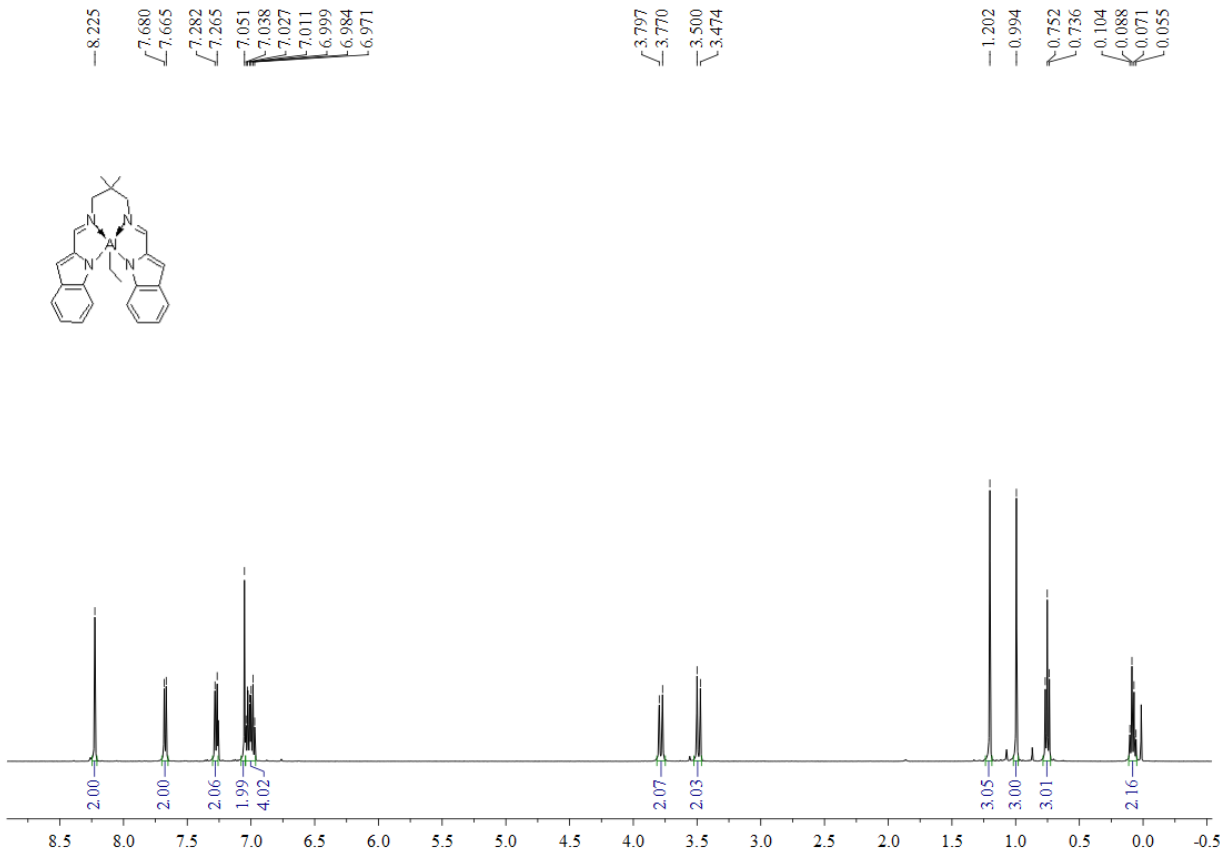

Figure S20. ^{1}H NMR spectrum (500 MHz, $CDCl_3$, 298 K) of complex **3**

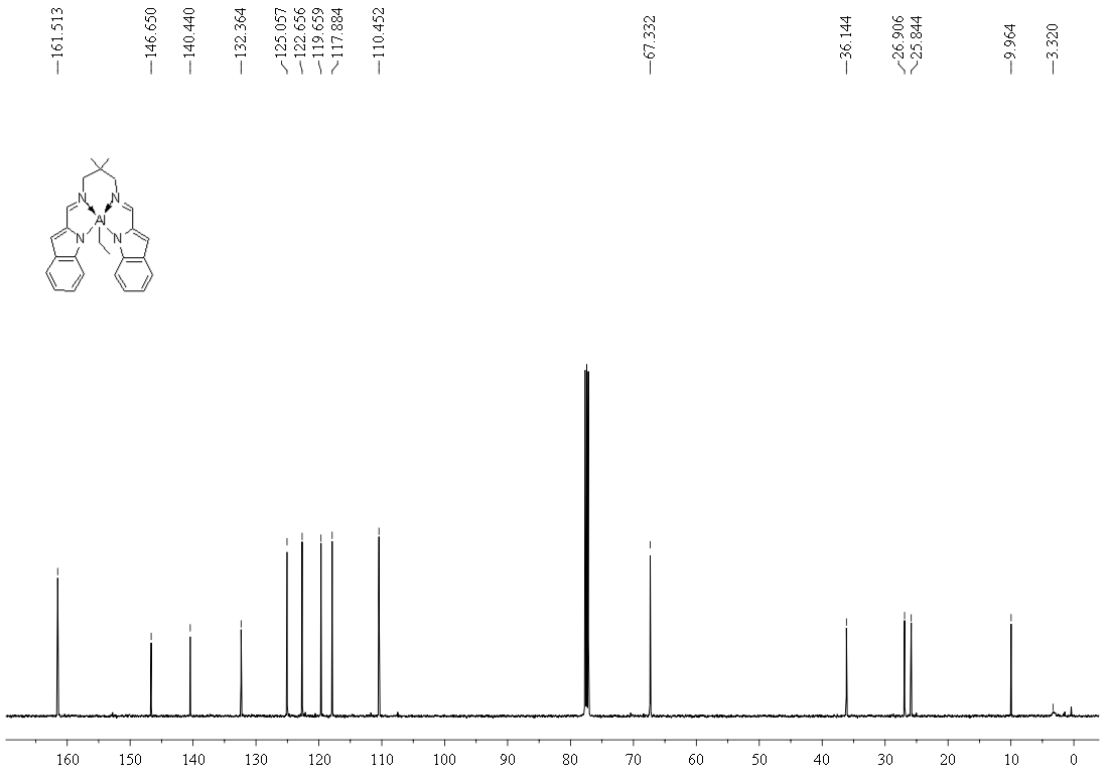

Figure S21. ^{13}C NMR spectrum (125 MHz, $CDCl_3$, 298 K) of complex **3**

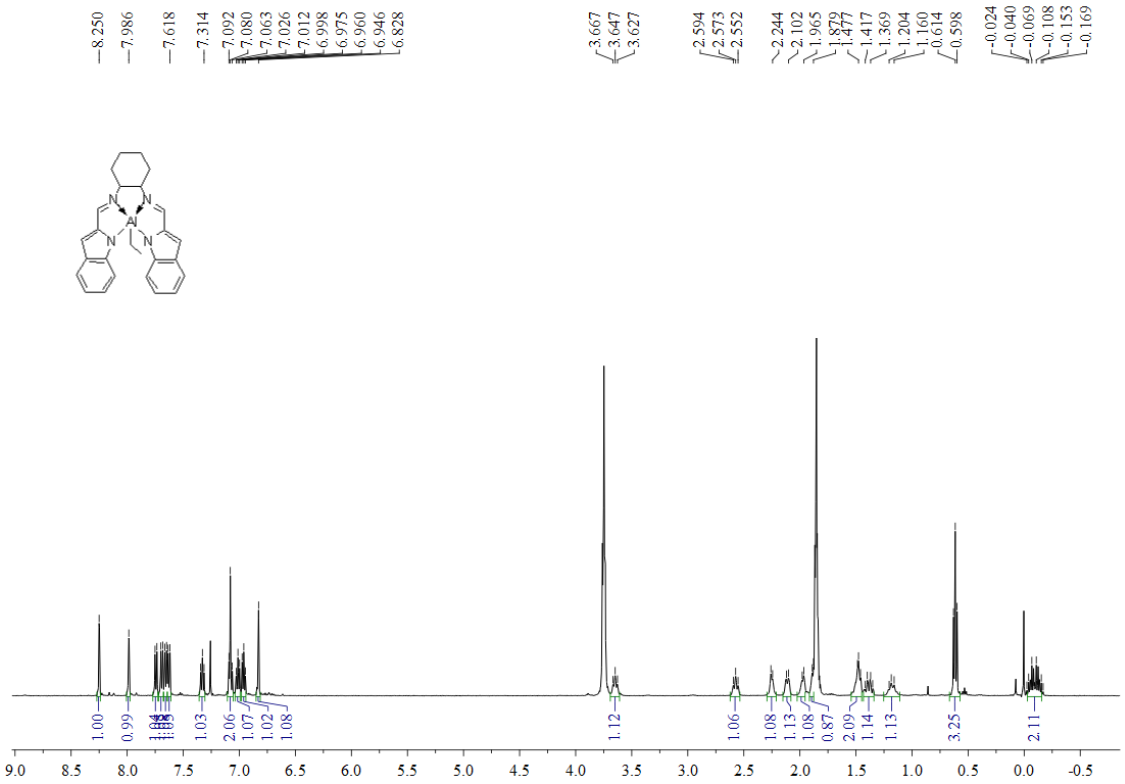

Figure S22. ^{1}H NMR spectrum (500 MHz, $CDCl_3$, 298 K) of complex **4**

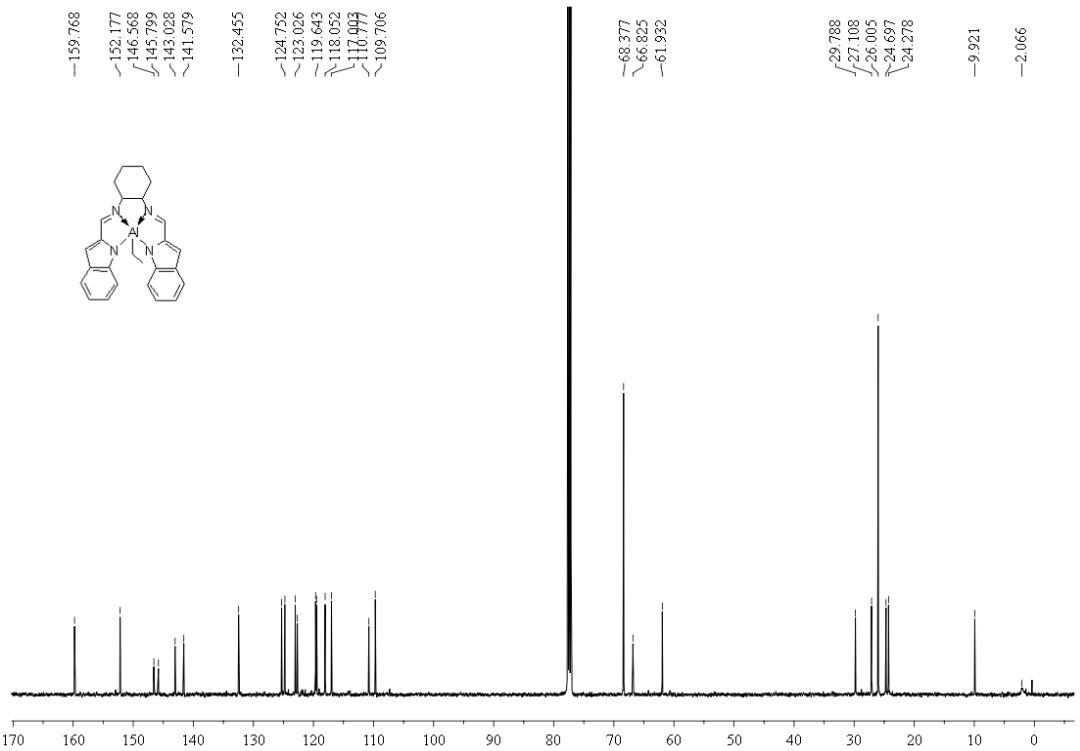

Figure S23. ^{13}C NMR spectrum (125 MHz, $CDCl_3$, 298 K) of complex **4**

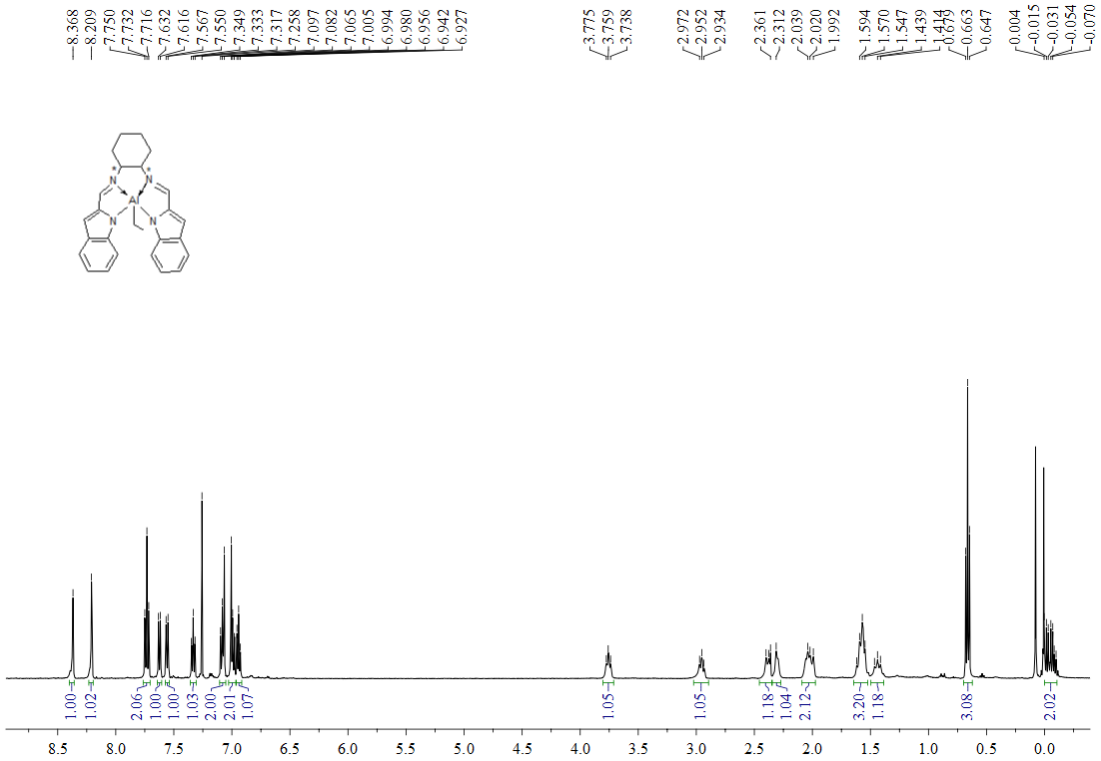

Figure S24. ^{1}H NMR spectrum (500 MHz, $CDCl_3$, 298 K) of complex **5**

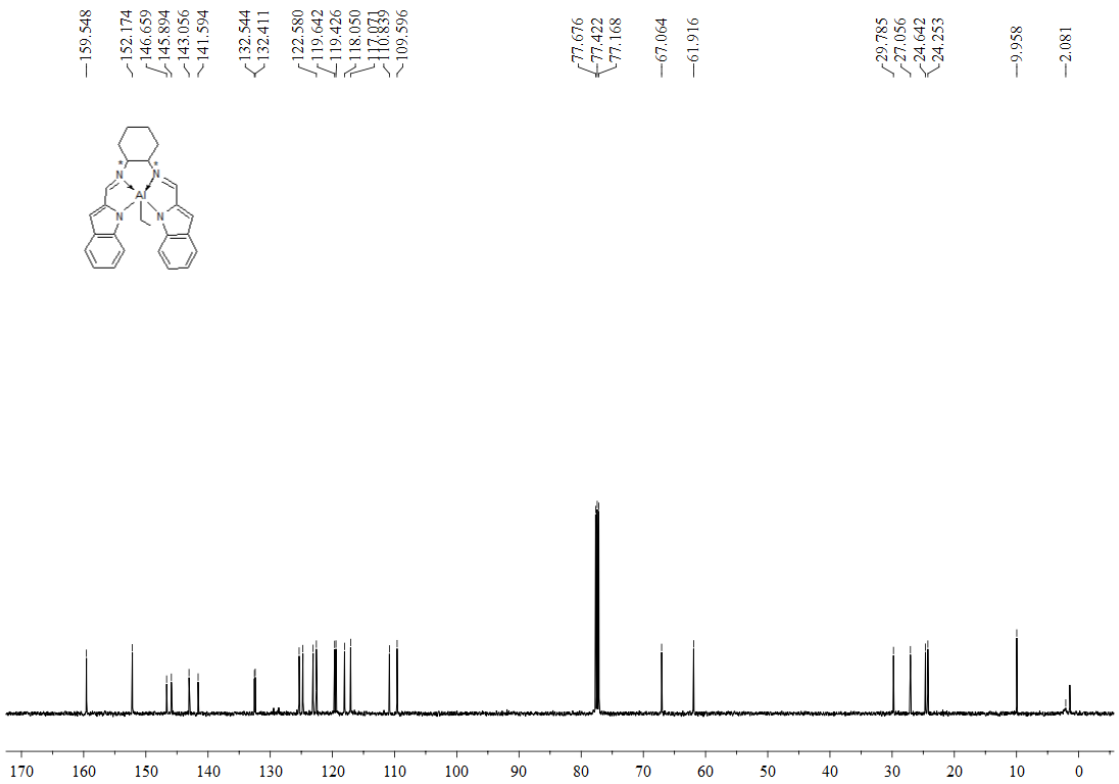

Figure S25. ^{13}C NMR spectrum (125 MHz, $CDCl_3$, 298 K) of complex **5**

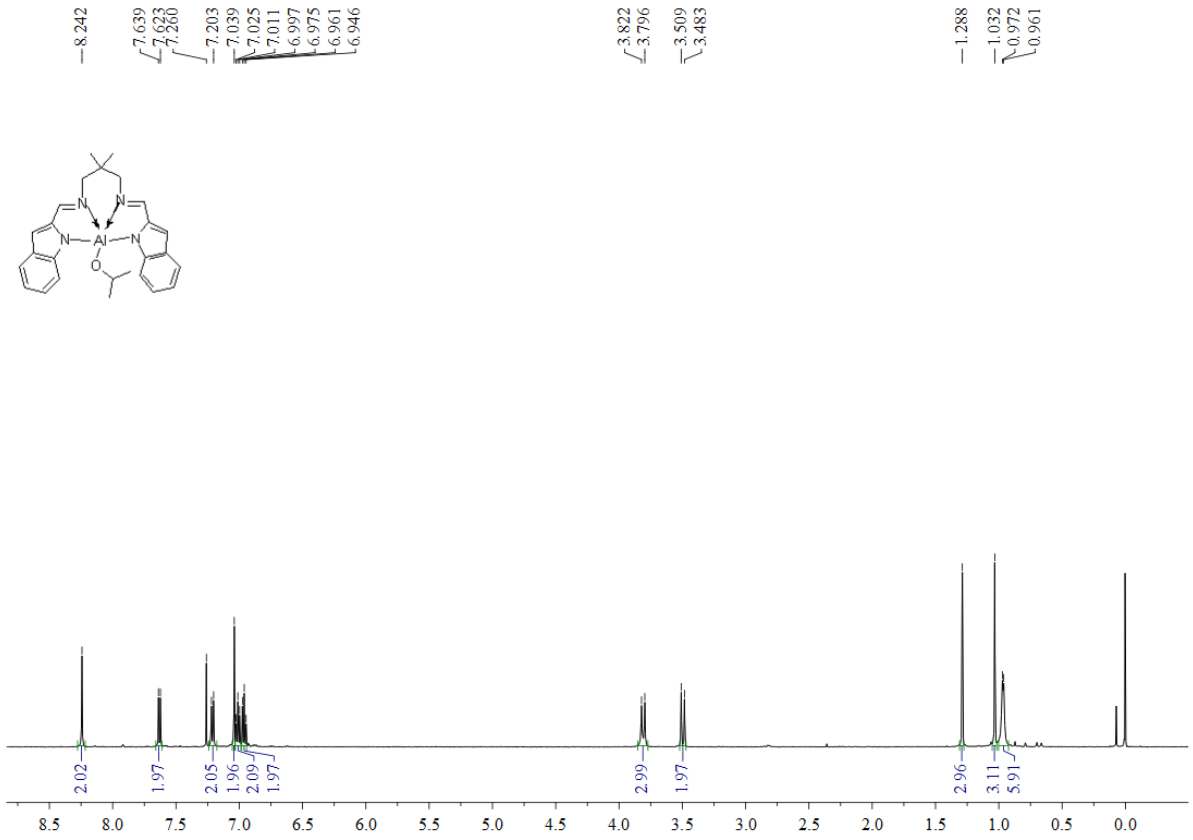

Figure S26. ^{1}H NMR spectrum (500 MHz, $CDCl_3$, 298 K) of complex **3a**

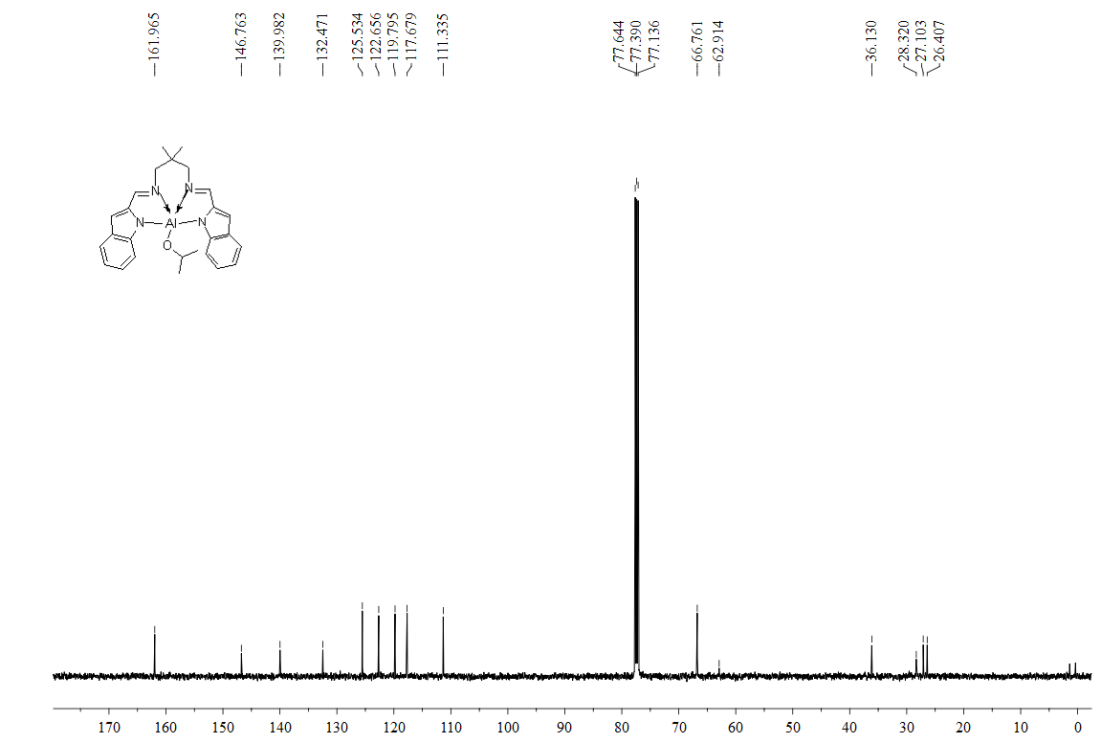

Figure S27. ^{13}C NMR spectrum (125 MHz, $CDCl_3$, 298 K) of complex **3a**

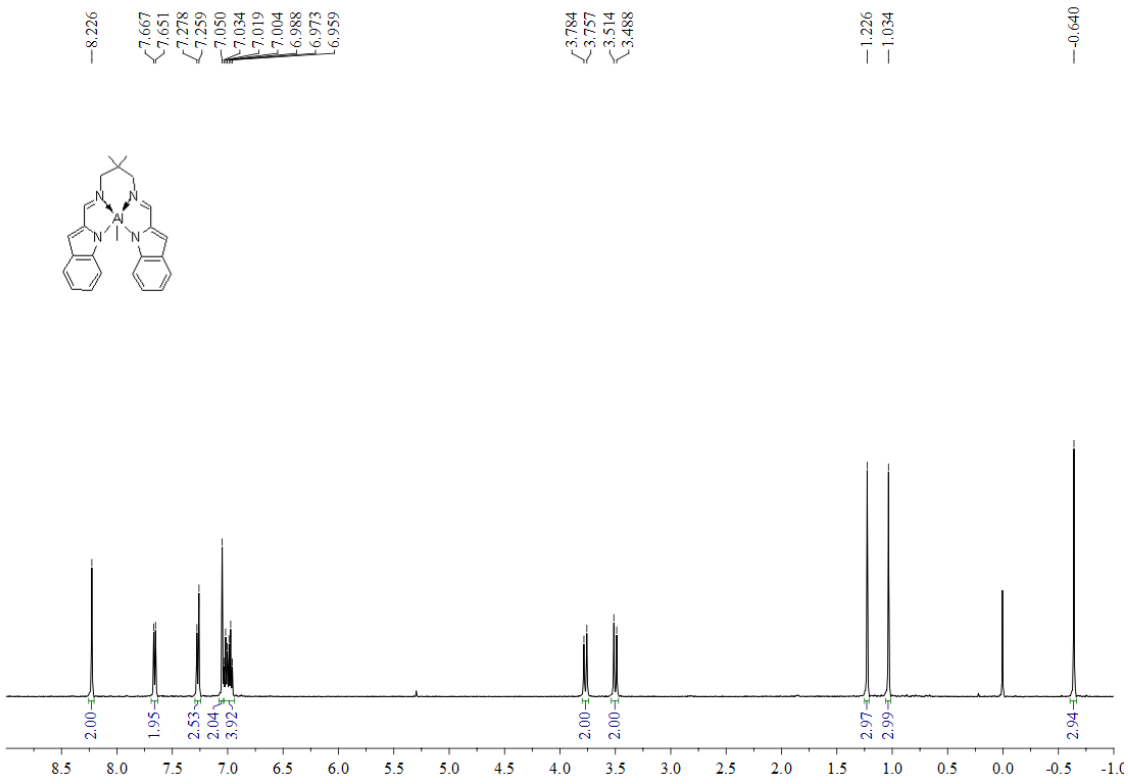

Figure S28. ^{1}H NMR spectrum (500 MHz, $CDCl_3$, 298 K) of complex **3b**

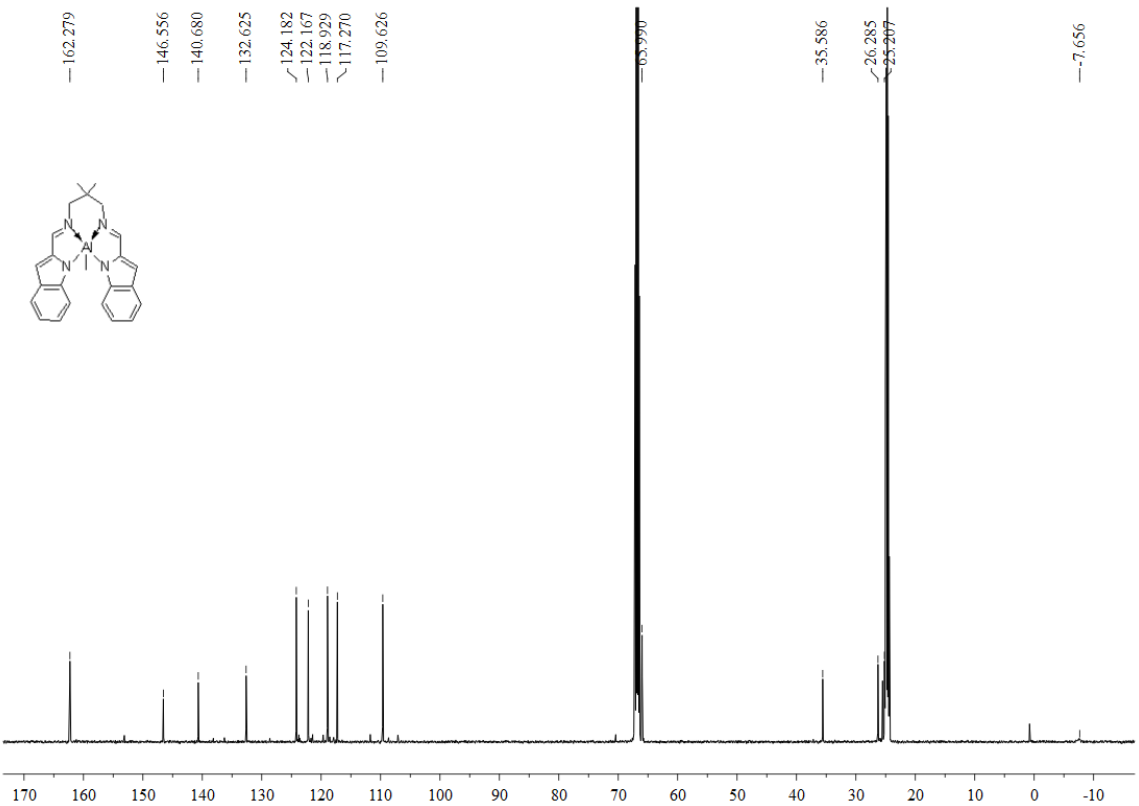

Figure S29. ^{13}C NMR spectrum (125 MHz, THF-d_8, 298 K) of complex **3b**

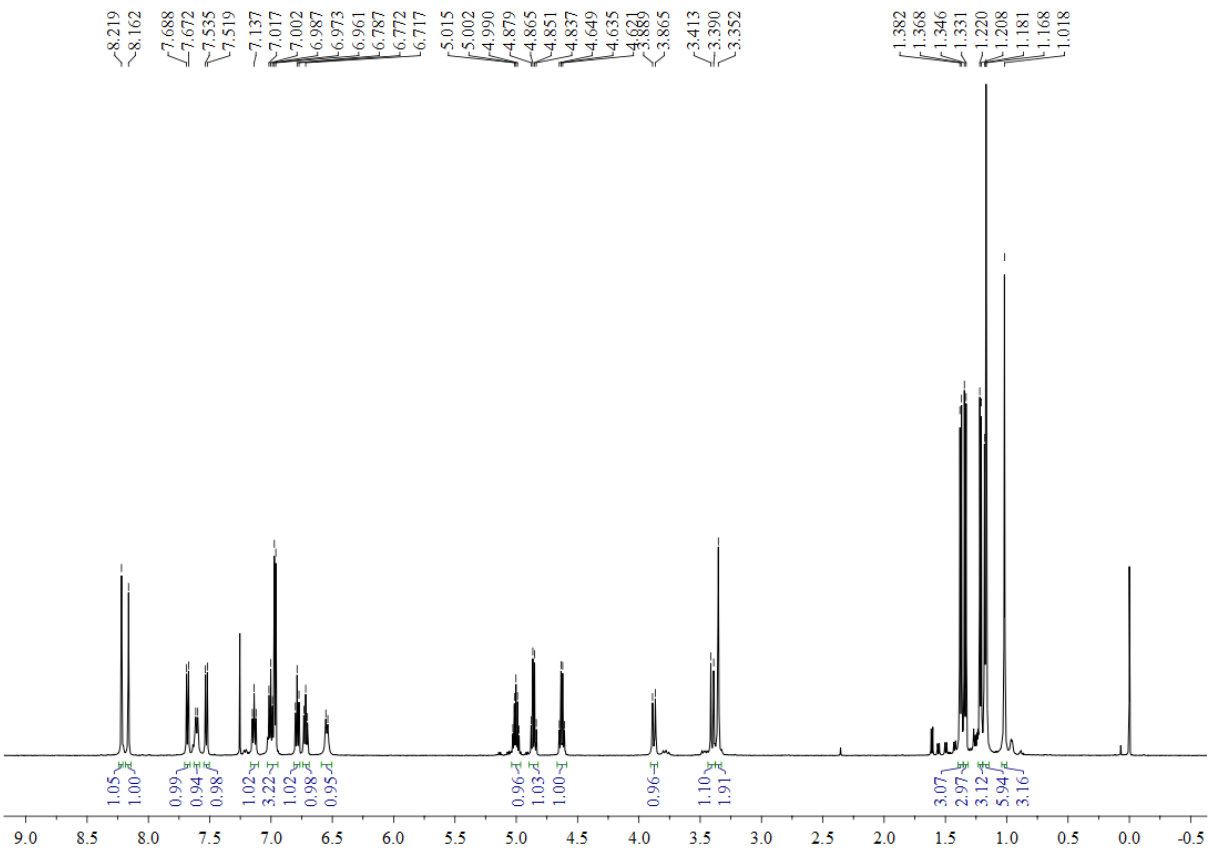

Figure S30. ^{1}H NMR spectrum (500 MHz, $CDCl_3$, 298 K) of complex **3c**

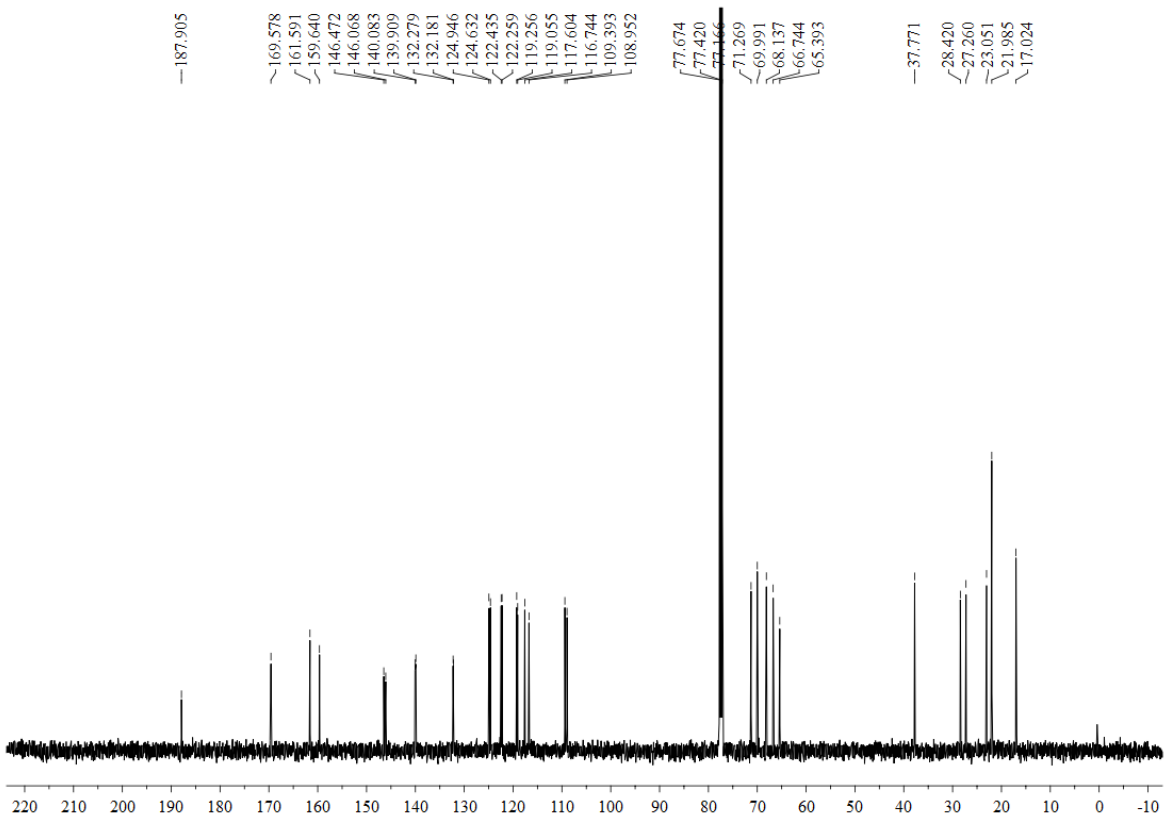

Figure S31. ^{13}C NMR spectrum (500 MHz, $CDCl_3$, 298 K) of complex **3c**

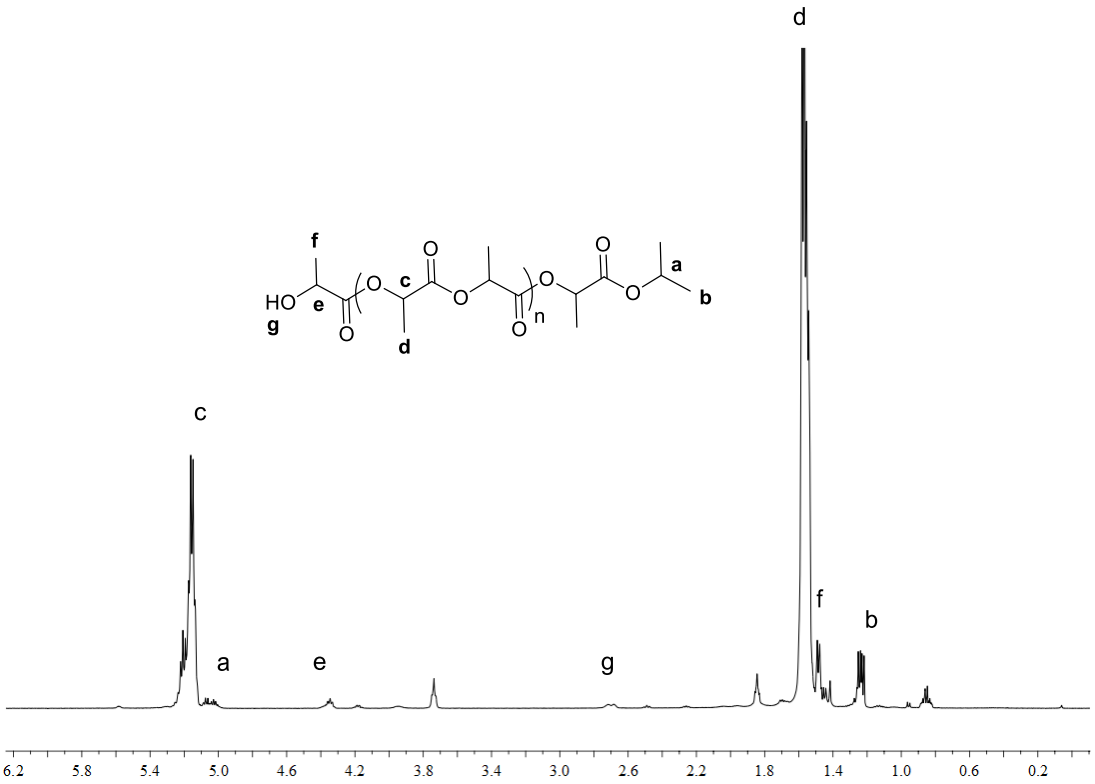

Figure S32. ^{1}H NMR spectrum (500 MHz, $CDCl_3$) of the *rac*-LA oligomer produced by complex **3** in the isopropanol ([*rac*-LA] : [**3**] : [OH] = 20 : 1 : 1, in toluene).

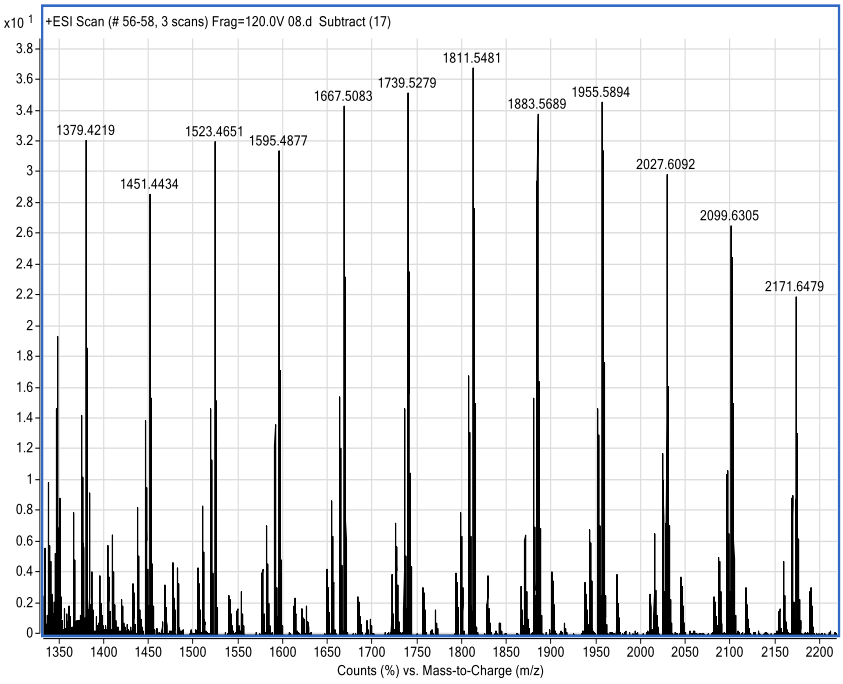

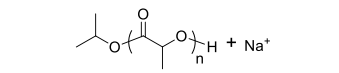

59.0497 72.0211 1.0078 22.9898

mass = 72.0211n + 59.0497 + 1.0078 + 22.9898

n	mass
18	1379.4219
19	1451.4434
20	1523.4651
21	1595.4877
22	1667.5083
23	1739.5279
24	1811.5481
25	1883.5689
26	1955.5894
27	2027.6092
28	2099.6305
29	2171.6479

Figure S33. ESI-TOF mass spectrum of the *rac*-LA oligomer produced by complex **3** in the isopropanol ([*rac*-LA] : [**3**] : [OH] = 20 : 1 : 1, in toluene).

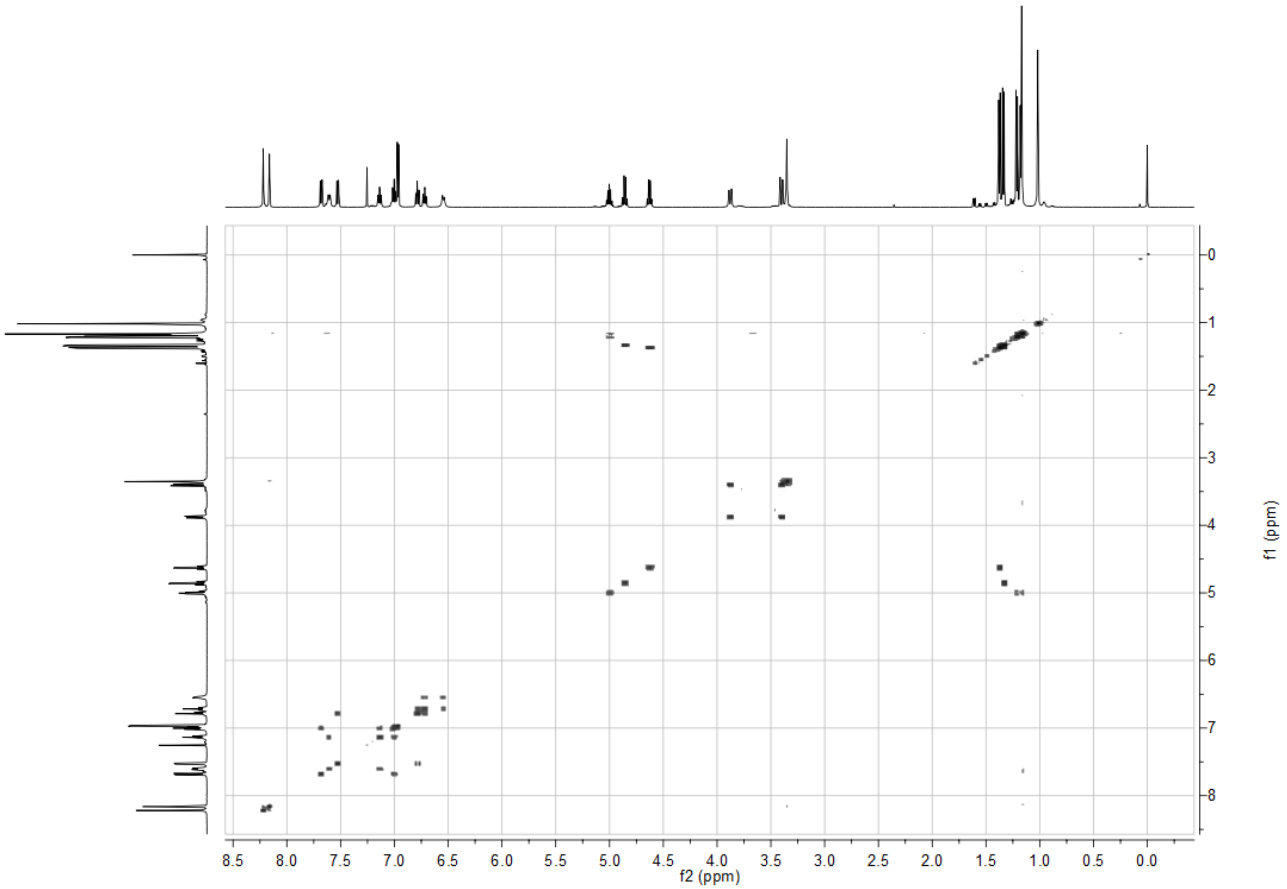

Figure S34. 2D NMR (^{1}H-^{1}H coupling) spectrum (500 MHz, $CDCl_3$, 298 K) data prepared from the reation of L-LA with **3a** (1 : 1).

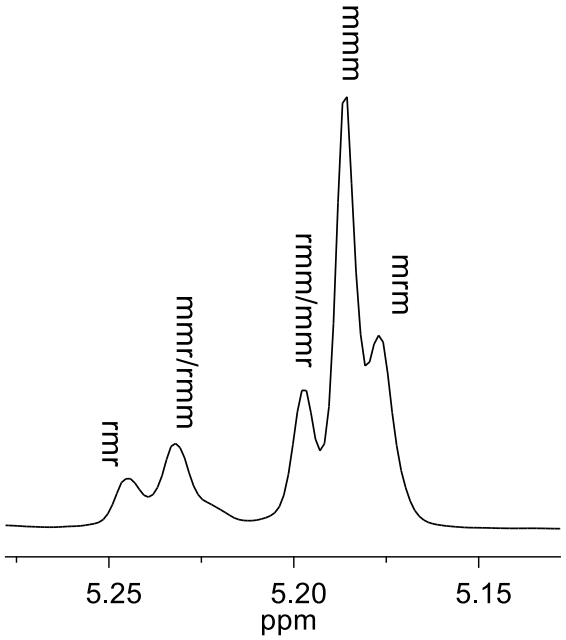

Figure S35. Homonuclear decoupled ^{1}H NMR spectrum of the methine region of PLA prepared from *rac*-lactide at 70 °C in toluene (500 MHz, $CDCl_3$) with **1**/2-propanol.

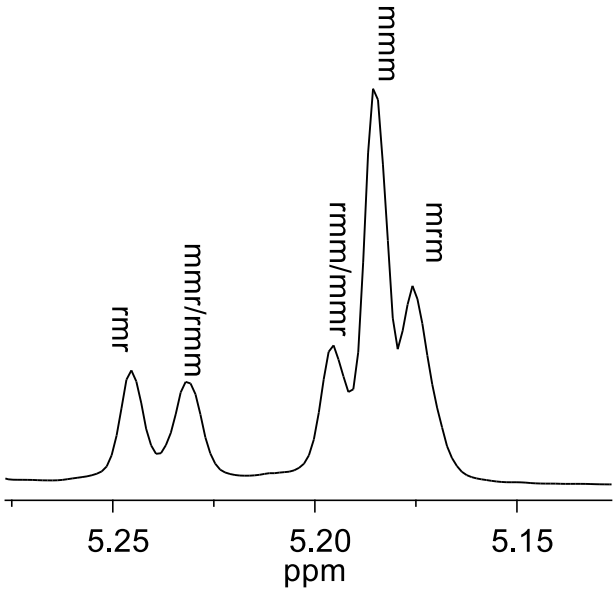

Figure S36. Homonuclear decoupled ^{1}H NMR spectrum of the methine region of PLA prepared from *rac*-lactide at 70 °C in toluene (500 MHz, $CDCl_3$) with **2**/2-propanol.

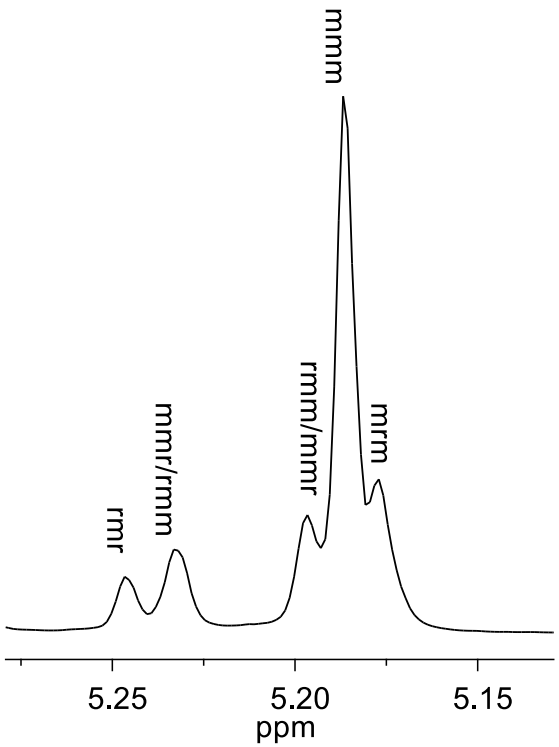

Figure S37. Homonuclear decoupled ^{1}H NMR spectrum of the methine region of PLA prepared from *rac*-lactide at 70 °C in toluene (500 MHz, $CDCl_3$) with **3**/2-propanol.

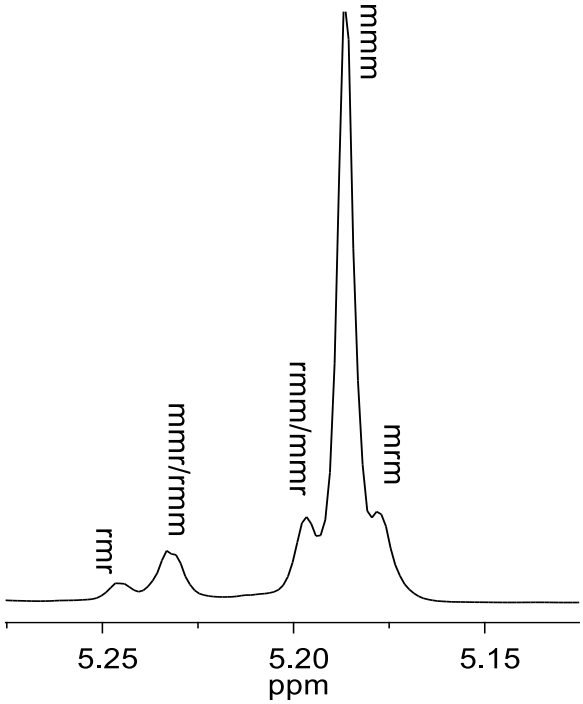

Figure S38. Homonuclear decoupled ^{1}H NMR spectrum of the methine region of PLA prepared from *rac*-lactide at 70 °C in toluene (500 MHz, $CDCl_3$) with **4**/2-propanol.

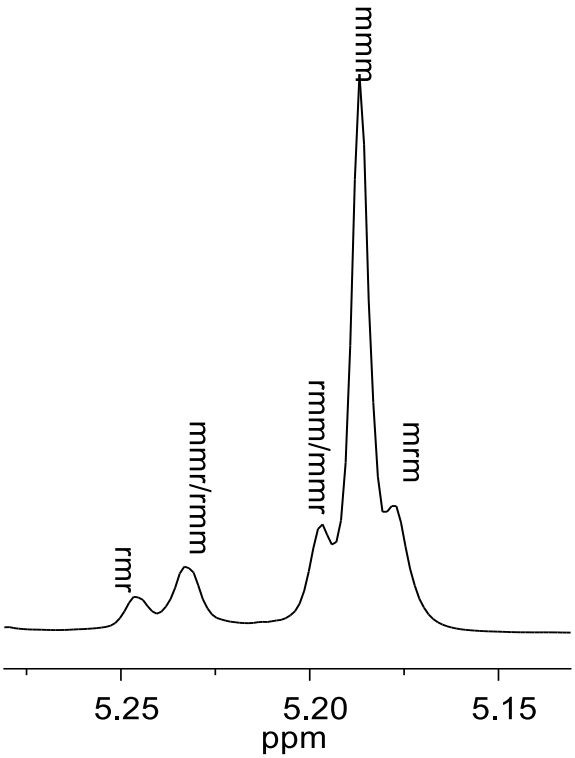

Figure S39. Homonuclear decoupled ^{1}H NMR spectrum of the methine region of PLA prepared from *rac*-lactide at 70 °C in toluene (500 MHz, $CDCl_3$) with **5**/2-propanol.

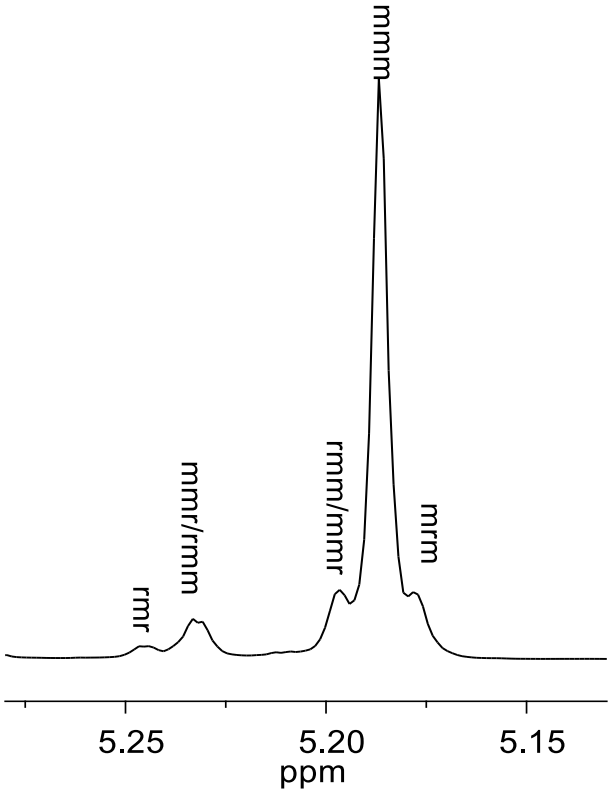

Figure S40. Homonuclear decoupled ^{1}H NMR spectrum of the methine region of PLA prepared from *rac*-lactide at 40 °C in toluene (500 MHz, $CDCl_3$) with **4**/2-propanol.

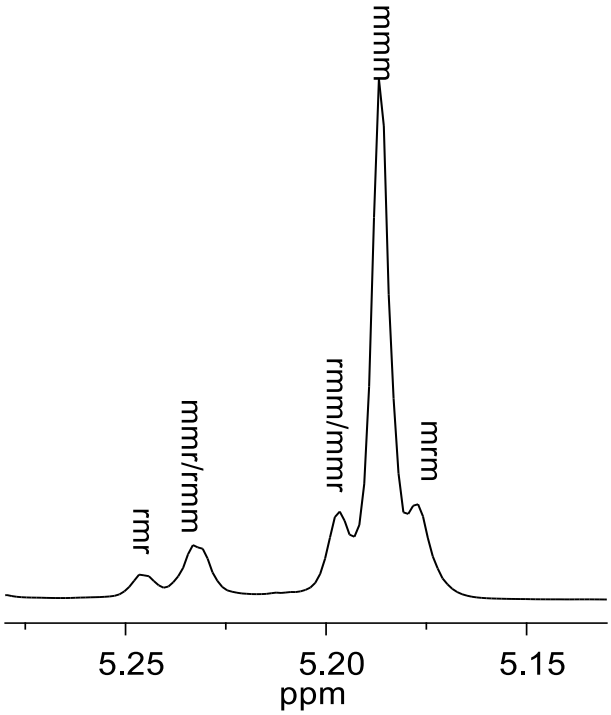

Figure S41. Homonuclear decoupled ^{1}H NMR spectrum of the methine region of PLA prepared from *rac*-lactide at 40 °C in toluene (500 MHz, $CDCl_3$) with **5**/2-propanol.

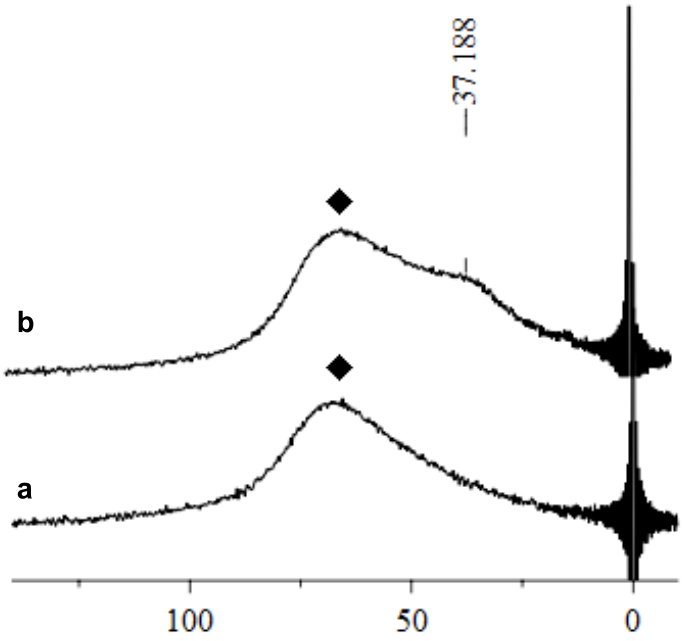

Figure S42. ^{27}Al NMR spectrum of **a**) an external solution of $Al(NO_3)_3$ and the ◆ indicate the probehead signal of blank sample; **b**) the reaction of L-LA with **3a** (1 : 1). (130.3 MHz, $CDCl_3$, r.t.)